A conservative discretization for the incompressible Navier-Stokes equation

Bachelor end project

Technische Universiteit Delft

Delft, 9 July 2024

Author: Hidde Wiefkers
Supervisors: Artur Palha & Bijoy Bera

Summary for laypersons

The Navier-Stokes equations are the physical laws which describe the movement of fluids. For most practical situations we don't have exact solutions to them and therefore we use computer simulations to describe the movements of fluids instead. These simulations are often made in a way were they divide space into smaller parts and compute simpler equations in these smaller spaces. This report focuses on one specific way to simulate the Navier-Stokes equations. What separates this way of simulating from others is that the conservation laws, which follow from the physical laws, are build into the underlying mathematics of this model in such a way that they are not dependant on the way the space is divided into smaller parts. This means that physical quantities, such as mass and energy, follow the physical laws for them no matter the way space is devided into smaller parts. This allows for simpler way of modeling complex shapes, while still keeping physically reasonable simulations. This is important, since for a lot of physical situations an extreme simplification is required, because otherwise even the most advanced computers can not simulate the fluid flow in any reasonable time. The conservation of these physical quantities should lead to a more physically realistic simulation in these simplified models and the results do support this conclusion.

In this report we first discuss some of the math required for this simulation and after that we analyse and discuss some results from this simulation.

Summary for peers

In[**?**] this report we implement and test a discretization for the 2D dimensionless incompressible Navier-Stokes equations, as described by Zhang, Palha, Gerritsma and Yao [19]. This discretization conserves mass, energy, enstrophy and vorticity. This discretization uses the finite element method. Which is a numerical method, which solves the problem by dividing the spatial domain into smaller sections and approximating the solution in these smaller parts using a linear combination of some chosen functions. One of these sections of space, together with the functions used for the approximation defined in it is called an element. The function spaces for these elements are picked in such a way as to preserve some structural characteristics of the differential equations. This is done by using a concept of differential geometry (and functional analysis) called the De Rahm complex.

We implement this discretization for the Navier-Stokes equations and apply it to the lid driven cavity problem. The lid driven cavity problem consists of a square box with non slip boundaries that is filled with fluid which is at rest. When suddenly the top of the box starts moving with a constant velocity to the left. For a sufficiently small Reynolds number and after sufficient time this should produce a steady state vortex. We compare the resulting steady state from this discretization against some highly resolved benchmarks and see that the method performs well. We then compare the discretization against the Taylor-Hood method for some initial times, before reaching a steady state and see that the discretization preforms better and importantly shows significantly smaller nonphysical oscilations.

Contents

1 Introduction

In this report we implement and test a discretization for the 2D dimensionless incompressible Navier-Stokes equations, as described by Zhang, Palha, Gerritsma and Yao [19]. This discretization conserves mass, energy, enstrophy and vorticity. It is constructed using the finite element method. The function spaces for these elements are picked in such a way as to preserve some structural characteristics of the differential equations. This is done by using a concept of differential geometry (and functional analysis) called the De Rahm complex. We first implemented this discretization in the programming language Julia [3], using the Gridap module [2] [18], due to the early stages of development of Gridap and the specificity of this method, the resulting discretization was slower than expected. We then implemented the discretization in Python, using the more mature Firedrake library [8], which resulted in computation times more in line with expectation.

The Navier-Stokes equations model the movement of fluids and have many important applications. In meteorology they are used for weather prediction [13] and in engineering they are used for the study of aerodynamic designs [10]. Exact solutions for these equations have only been found for some very specific cases, such as steady state flow in a cylinder or with specific periodic spatial conditions [6]. This means that in most practical situations an exact solution is not known and a numerical approximation is necessary.

A challenge in numerical approximations for the Navier-Stokes equations is to compute an accurate simulation in practical times. A key ingredient for physical fidelity is to capture/reproduce the correct energy spectrum and it's cascade. If the numerical approximation is done incorrectly too much of the energy can dissipate or the solution can blow up. Both of these situations create unphysical results. A discretization, which conserves the relevant physical quantities should more accurately describe this energy spectrum, even for the very under resolved case.

It has been suggested that secondary conservation properties, meaning conservation of derived quantities which are not directly unknowns, could improve physical fidelity in numerical methods [16]. But numerical methods, which include secondary conservation properties do not address all kinds of spurious solutions [16]. Numerical methods that satisfy fundamental mathematical identities e.g. the divergence of the curl is equal to zero and the curl of the gradient is equal to zero can, however, exactly preserve physical properties, such as divergence free properties or gradient free properties [16][1]. Also for the Navier-Stokes equations, there has been written about secondary conservation properties leading to better results [5].

In this report we gradually build up to the discretization for the Navier-Stokes equation. We do so by introducing the theory required alongside working out examples. These examples will be of the heat equation, which is not related to the Navier-Stokes equation in the underlying physics. But with these examples we introduce the mathematical building blocks required for the discretization of the Navier-Stokes equation. First we introduce the weak form, along side an example for the primal form steady heat equation. Then we illustrate the De Rahm complex and how to work with multiple unknowns with an example of the mixed form steady heat equation. After this we introduce the finite element method and apply it to these two examples. Lastly we explain how to solve a transient problem, using the primal form unsteady heat equation as an example.

We will first briefly discuss the finite element method and the de Rahm complex in Chapter 2. We will illustrate this theory by working out two examples, those of the Primal and the Mixed form heat equation. We then apply the finite element method to the incompressible dimensionless Navier-Stokes equations and discuss it's conservation properties in chapter 3. In chapter 4 we discuss the results from implementing the worked out examples in the Julia programming language[3], using the Gridap[2][18] module and the results from implementing the Navier-Stokes equations in Python, using the Firedrake library[8].

2

A brief introduction to the finite element method

In this chapter we discuss the theoretical background for the conservative discretization of the Navier-Stokes equations we are studying. We first introduce the types of problems we analyse, in Section 2.1. Following this we introduce an alternative formulation for these problems, which is called the weak form in Section 2.2. Then we briefly discuss the function spaces used in this report and introduce the de Rahm complex in Section 2.3. Finally, we describe how to use the finite element method in Section 2.4.

2.1. Strong form

Boundary value problems are differential equations which are defined in a given region and are subject to constraints on the boundary of that region. These problems can be expressed as follows:

$$\begin{aligned} &\text{Find } u \in U \text{ such that} \\ &\begin{cases} \mathscr{L}[u] = 0 \text{ in } \Omega, \\ + \text{ appropriate boundary conditions on } \partial\Omega. \end{cases} \end{aligned} \tag{2.1}$$

Where $\mathscr{L}$ is a differential operator, Ω is the region in which the differential equation is defined, $\partial\Omega$ is the boundary of Ω, u is the solution to the problem, which can be either a vector or a scalar function, and U is the solution function space with sufficient regularity such that the operator $\mathscr{L}$ is well defined and the solution u exists. The differential equation (2.1) is called the *strong form* of the boundary value problem.

2.2. Weak form

In order to solve these problems with the finite element method (see Section 2.4), we first have to rewrite them in their *weak form* [9, p. 4-6], which is a generalization of the problem.

$$\begin{aligned} &\text{Find } u \in U^w, \text{ such that} \\ &\begin{cases} \langle \mathscr{L}[u], v \rangle_\Omega = 0, & \forall v \in V^w, \\ + \text{appropriate boundary conditions on } \partial\Omega, \end{cases} \end{aligned} \tag{2.2}$$

where $\langle a, b \rangle_\Omega := \int_\Omega a \cdot b \, \mathrm{d}\Omega$ and we pick the solution space U^w and test space V^w such that they have sufficient regularity[1] for these equations to be meaningful[2].

For these equations to be meaningful, we need

$$|\langle \mathscr{L}[u], v \rangle_\Omega| < \infty, \quad \forall v \in V^w \text{ and } \forall u \in U^w. \tag{2.3}$$

[1] With "regularity" we mean that the spaces contain functions that are differentiable, such that the differtial operator is well defined and the required integrals over Ω converge.

[2] With "meaningful" we mean that the required integrals converge and that the solutions exist.

By Schwartz's inequality [17, p. 24],

$$|\langle \mathscr{L}[u], v\rangle_\Omega| \leq \|\mathscr{L}[u]\|_\Omega \|v\|_\Omega, \tag{2.4}$$

where $\|a\|_\Omega^2 := \langle a, a\rangle_\Omega$. By equations (2.3) and (2.4) we have that for the integral present in our weak form to be meaningful, we need to have

$$\|\mathscr{L}[u]\|_\Omega < \infty \quad \text{and} \quad \|v\|_\Omega < \infty. \tag{2.5}$$

Therefore, we pick the spaces U^w and V^w such that

$$U^w := \{u : \|\mathscr{L}[u]\| < \infty\}, \quad \text{and} \quad V^w = L^2(\Omega) := \{v : \|v\|_\Omega < \infty\}. \tag{2.6}$$

It is important to note that if a function $u \in U^w$ satisfies equations (2.2), then, by the fundamental lemma of the calculus of variations [11, p. 9], u satisfies equation (2.1). This gives us a different starting point to find solutions to the problem (2.1).

The condition $u \in U^w$ is quite restrictive for certain boundary value problems, particularly so in the context of the finite element method. In order to loosen this restriction, and thus find approximate solutions, we need to introduce the concept of *weak differential operator* $\widetilde{\mathscr{L}}$. Where $\widetilde{\mathscr{L}}[u] = \mathscr{L}[u]$ for $u \in U^w$. This allows us to look for solutions in a wider space $\widetilde{U}$, for which $\widetilde{\mathscr{L}}[u]$ for $u \in \widetilde{U}$ is still properly defined, while $\mathscr{L}[u]$ is no longer properly defined. If the weak differential operator is properly chosen then $U \subset \widetilde{U}$. This weak differential operator is obtained by using integration by parts on one or multiple high order differentials that make up the differential operator.

In this project we focus on problems in two dimensions. Important differential operators in 2D are the gradient, $\nabla u := \frac{\partial u}{\partial x}\vec{e}_x + \frac{\partial u}{\partial y}\vec{e}_y$, the rotor, $\nabla \times \vec{u} := \frac{\partial}{\partial x}(\vec{u}\cdot\vec{e}_y) - \frac{\partial}{\partial y}(\vec{u}\cdot\vec{e}_x)$, the divergence, $\nabla\cdot\vec{u} := \frac{\partial}{\partial x}(\vec{u}\cdot\vec{e}_x) + \frac{\partial}{\partial y}(\vec{u}\cdot\vec{e}_y)$, and the curl, $\nabla_\perp := -\frac{\partial}{\partial y}\vec{e}_x + \frac{\partial}{\partial x}\vec{e}_x$. Where $\vec{e}_x$ and $\vec{e}_y$ are the unit vectors pointing in in the x and y direction, respectively and the arrow, $\vec{}$, means it is a vector in 2 dimensions. These differential operators are associated with the following spaces:

$$H^1(\Omega) = \left\{ u \in L^2(\Omega) : \int_\Omega \nabla u \cdot \nabla u \, \mathrm{d}\Omega < \infty \right\}, \tag{2.7}$$

$$H(\mathrm{rot},\Omega) = \left\{ \vec{u} \in [L^2(\Omega)]^2 : \int_\Omega (\nabla \times \vec{u}) \cdot (\nabla \times \vec{u}) \mathrm{d}\Omega < \infty \right\}, \tag{2.8}$$

$$H(\mathrm{div},\Omega) = \left\{ \vec{u} \in [L^2(\Omega)]^2 : \int_\Omega (\nabla \cdot \vec{u})(\nabla \cdot \vec{u}) \mathrm{d}\Omega < \infty \right\}, \tag{2.9}$$

$$H(\mathrm{curl},\Omega) = \left\{ u : u \in L^2(\Omega), \int_\Omega (\nabla_\perp u) \cdot (\nabla_\perp u) \, \mathrm{d}\Omega < \infty \right\}. \tag{2.10}$$

Note that for functions in H^1 it holds that these functions and their gradient are integrable, for functions in $H(\mathrm{rot},\Omega)$ it holds that these functions and their rotor are integrable, etc. All the differential operators also have an associated weak operator. They are defined as follows.

The *weak gradient*, $\widetilde{\nabla} : L^2(\Omega) \mapsto H(\mathrm{div},\Omega)$, acting on $u \in L^2(\Omega)$, is defined as

$$\langle \widetilde{\nabla} u, \vec{v}\rangle_\Omega = -\langle u, \nabla\cdot\vec{v}\rangle_\Omega + \int_{\partial\Omega} u(\vec{v}\cdot\vec{n}) d\Gamma, \quad \forall \vec{v} \in H(\mathrm{div},\Omega). \tag{2.11}$$

The *weak divergence*, $\widetilde{\nabla}\cdot : H(\mathrm{rot},\Omega) \mapsto H^1(\Omega)$, acting on $\vec{u} \in H(\mathrm{rot},\Omega)$, is defined as

$$\langle \widetilde{\nabla}\cdot\vec{u}, v\rangle_\Omega = -\langle u, \nabla v\rangle_\Omega + \int_{\partial\Omega} v(\vec{u}\cdot\vec{n}) d\Gamma, \qquad \forall v \in H^1(\Omega). \tag{2.12}$$

The *weak rotor*, $\widetilde{\nabla\times} : H(\mathrm{div},\Omega) \mapsto H(\mathrm{curl},\Omega)$, acting on $\vec{u} \in H(\mathrm{div},\Omega)$, is defined as

$$\langle \widetilde{\nabla\times}\vec{u}, v\rangle_\Omega = \langle u, \nabla_\perp v\rangle_\Omega - \int_{\partial\Omega} v(\vec{u}\times\vec{n}) d\Gamma, \qquad \forall v \in H^1(\Omega). \tag{2.13}$$

Finally, the *weak curl*, $\widetilde{\nabla_\perp} : L^2(\Omega) \mapsto H(\mathrm{rot},\Omega)$, acting on $u \in L^2(\Omega)$, is defined as

$$\langle \widetilde{\nabla_\perp} u, \vec{v}\rangle_\Omega = \langle u, \nabla\times\vec{v}\rangle_\Omega + \int_{\partial\Omega} u(\vec{v}\times\vec{n}) d\Gamma, \qquad \forall \vec{v} \in H(\mathrm{rot},\Omega). \tag{2.14}$$

Where $\vec{n}$ is the outward pointing unit normal vector. Note that the function spaces used in the definitions of the weak differential operators provide the necessary conditions for the integrals to converge. For further discussion of these weak operators and that they are well posed see [7, p. 544].

These weak operators allow us to construct weak versions of our operator $\mathscr{L}$ and, in this way, relax the regularity constraints on the solution space. An important point to highlight is that, as seen before, a reduction in the regularity of the solution space U leads to a corresponding increase in the regularity of the test space V. This is expected since integration by parts transfers the differentiation from one term of integral (the solution) to the other term (the test function). If we apply these ideas to (2.2) we get

$$\begin{cases} \langle \widetilde{\mathscr{L}}[u], v\rangle_\Omega = 0\,, & \forall v \in \widetilde{V}\,, \\ u = g_E\,, \text{ on } \Gamma_E\,, \\ \mathscr{D}[u] = g_N\,, \text{ on } \Gamma_N\,, \end{cases} \tag{2.15}$$

where $u \in \widetilde{U}$ is a solution to our problem and $\widetilde{U}$ is the solution functions space with sufficient regularity such that the weak operator $\widetilde{\mathscr{L}}$ is well defined, Γ_E is the part of the boundary where *essential boundary conditions* are prescribed, Γ_N is the part of the boundary where *natural boundary conditions* are prescribed, $\Gamma_E \cup \Gamma_N = \partial\Omega$, $\Gamma_E \cap \Gamma_N = \emptyset$ and $\mathscr{D}$ is some (differential) operator and g_E and g_N are known functions.

As mentioned before, the boundary conditions can be of two types: essential or natural. Essential boundary conditions are typically directly enforced on the solution space itself, while natural boundary conditions are prescribed on the boundary integrals that appear when constructing the weak form of the equations. Note that, as indicated before, u can have both natural and essential boundary conditions at different parts of the boundary.

In order to clarify the ideas discussed so far, in the next subsection, we give a concrete example of how to construct the weak form for the case of the steady heat equation.

2.2.1. The primal form steady heat equation

To clarify the concepts just introduced, we will use as an example the primal form steady heat equation. The strong form of this is given by:

$$\begin{gathered} \text{find } u \in U \text{ such that} \\ \begin{cases} -\nabla\cdot\kappa\nabla u = f\,, & \text{in } \Omega\,, \\ u = g_E\,, & \text{on } \Gamma_E\,, \\ \kappa\nabla u\cdot\vec{n} = g_N\,, & \text{on } \Gamma_N\,, \end{cases} \end{gathered} \tag{2.16}$$

where $u \in U = C^2(\Omega)$ (twice continuously differentiable functions) is the temperature, κ is the material's heat conductivity, f represents heat sources (or sinks), and as usual $\vec{n}$ represents the outwards unit normal vector. At any point on the boundary either the temperature (u) or the heat flux ($\kappa\nabla u\cdot\vec{n}$) is prescribed. The temperature is directly prescribed onto the unknown u and this condition is therefore an essential boundary condition. The heat flux is prescribed onto u with a differential operator and is therefore a natural boundary condition. Recall that these boundary conditions can not overlap, $\Gamma_E \cap \Gamma_N = \emptyset$, and conditions need to be given for the entire boundary, $\Gamma_E \cup \Gamma_N = \partial\Omega$. For simplicity we will consider the case $\kappa = 1$.

Following the ideas presented before, these equations can be rewritten in the equivalent weak form

$$\begin{gathered} \text{Find } u \in U^w = H^2(\Omega) \text{ such that} \\ \begin{cases} -\langle \nabla\cdot\nabla u, v\rangle_\Omega = \langle f, v\rangle_\Omega\,, & \forall v \in V^w = L^2(\Omega)\,, \\ u = g_E\,, & \text{on } \Gamma_E\,, \\ \nabla u\cdot\vec{n} = g_N\,, & \text{on } \Gamma_N\,, \end{cases} \end{gathered} \tag{2.17}$$

where

$$H^2(\Omega) := \left\{ u \in L^2(\Omega) : \|\nabla u\|_\Omega < \infty \quad \text{and} \quad \|\nabla\cdot\nabla u\|_\Omega < \infty \right\}. \tag{2.18}$$

Since f and Ω are assumed to be finite, we have that $\|f\|_\Omega < \infty$. Additionally, note that in this case $\mathscr{L}[u] = f + \nabla\cdot\nabla u$. By the triangle inequality [17, p. 24], $\|f + \nabla\cdot\nabla u\|_\Omega \le \|f\|_\Omega + \|\nabla\cdot\nabla u\|_\Omega$. This means that the condition $\|\mathscr{L}[u]\|_\Omega < \infty$ is satisfied, when $u \in H^2(\Omega)$. Therefore $u \in H^2(\Omega) = U^w$, as it is described previously.

To loosen the requirement $u \in H^2(\Omega)$ we can employ the weak divergence operator $\widetilde{\nabla}$ (2.12), and rewrite (2.17) as,

$$\text{Find } u \in \widetilde{U}_E, \text{ such that}$$
$$\langle \nabla u, \nabla v \rangle_\Omega - \int_{\Gamma_N} g_N v \, \mathrm{d}\Gamma_N = \langle f, v \rangle_\Omega, \forall v \in \widetilde{V}_0, \tag{2.19}$$

where

$$\widetilde{U}_E := \left\{ u \in \widetilde{U} = H^1(\Omega) : \; u|_{\Gamma_E} = g_E \right\}, \tag{2.20}$$

and

$$\widetilde{V}_0 := \left\{ v \in \widetilde{V} = H^1(\Omega) : \; v|_{\Gamma_E} = 0 \right\}. \tag{2.21}$$

Using the notation introduced before, we can rewrite (2.19) in an alternative form

$$\text{Find } u \in \widetilde{U}_E, \text{ such that}$$
$$-\langle \widetilde{\nabla} \cdot \nabla u, v \rangle_\Omega = \langle f, v \rangle_\Omega, \forall v \in \widetilde{V}_0. \tag{2.22}$$

Note three important aspects:
(i) By employing the weak divergence $\widetilde{\nabla}\cdot$ we were able to reduce the regularity requirements on the solution space $\widetilde{U}$ at the expense of an increased regularity on the test space $\widetilde{V}$. $H^1(\Omega)$ is the space in which our weak differential operator [3] is properly defined. And indeed $H^1(\Omega) \supset H^2(\Omega)$.

(ii) We have directly imposed the essential boundary conditions (the ones over Γ_E) on the solution space $\widetilde{U}_E$ and correspondingly on the test space $\widetilde{V}_0$ and included the natural boundary conditions (the ones over Γ_N) on the boundary integral that appears from the definition of the weak divergence. This highlights the *essential* and *natural* character of the two types of boundary conditions.

(iii) Note that $\langle \widetilde{\nabla} \cdot \nabla u, v \rangle_\Omega = \langle \nabla \cdot \nabla u, v \rangle_\Omega$ if u is sufficiently smooth. This can be shown through integration by parts.

2.3. The de Rham complex

In equations (2.6) and (2.7) we introduced the function spaces used in this work. Typically, these spaces are considered in isolation, i.e., without a direct relation between them. This is particularly the case when considering their discrete counterparts. Despite this usual approach, there is an underlying relation between the different spaces. These relations have been identified as essential for the construction of stable numerical discretisations [1] [7]. In this section we will identify and discuss these relations and the structure they form, the De Rham complex.

Note that that if $u \in H(\mathrm{curl}, \Omega)$, then, by definition $\nabla_\perp u \in [L^2(\Omega)]^2$ and $\nabla \cdot (\nabla_\perp \vec{u}) = 0 \in L^2(\Omega)$. Therefore if $u \in H(\mathrm{curl}, \Omega)$, then $\nabla_\perp u \in H(\mathrm{div}, \Omega)$ and $\nabla \cdot (\nabla_\perp u) = 0$. Also By definition of $H(\mathrm{div}, \Omega)$, if $\vec{u} \in H(\mathrm{div}, \Omega)$, then $\nabla \cdot \vec{u} \in L^2(\Omega)$. This means that these spaces form a sequence, where a differential operator maps a space into the next space, specifically in the nul space of the next differential operator. This sequence, together with the operators, is called an *exact sequence*, which is a type of de Rahm complex.

$$\mathbb{R} \rightarrow H(\mathrm{curl}, \Omega) \xrightarrow{\nabla_\perp} H(\mathrm{div}, \Omega) \xrightarrow{\nabla\cdot} L^2(\Omega) \rightarrow 0^4. \tag{2.23}$$

Furthermore if $u \in H^1(\Omega)$ then $\nabla u \in [L^2(\Omega)]^2$ and $\nabla \times \nabla u = 0$. Therefor if $u \in H^1(\Omega)$, then $\nabla u \in H(\mathrm{rot}, \Omega)$ and $\nabla \times \nabla u = 0 \in L^2(\Omega)$. Also, by definition, if $u \in H(\mathrm{rot}, \Omega)$, then $\nabla \times u \in L^2(\Omega)$. This means that these spaces form a second exact sequence

$$\mathbb{R} \rightarrow H^1(\Omega) \xrightarrow{\nabla} H(\mathrm{rot}, \Omega) \xrightarrow{\nabla\times} L^2(\Omega) \rightarrow 0. \tag{2.24}$$

[3] While $\widetilde{\nabla}$ is a weak operator, using the notation in section 2.2 our weak operator for this problem is $\widetilde{\mathscr{L}}[u] = \widetilde{\nabla} \cdot \nabla[u] + f$.

[4] Where $\mathbb{R} \rightarrow$ and $\rightarrow 0$ are added to complete the exact sequence. $\mathbb{R} \rightarrow H(\mathrm{curl}, \Omega)$ can be thaught of as being a mapping from the reals to the function space with only constant functions. So that all these functions are in the null space of $H(\mathrm{curl}, \Omega)$. $L^2(\Omega) \rightarrow 0$ can be taught of as adding an operator such that $\nabla\cdot$ maps functions in $H(\mathrm{div}, \Omega)$ to the nullspace in $L^2(\Omega)$. For further explanation see [7]

The weak differential operators defined in section 2.2 work similarly. By the definition of the weak gradient, if $u \in L^2(\Omega)$, then $\tilde{\nabla} u \in H(\mathrm{div}, \Omega)$. And if $\vec{u} \in H(\mathrm{div}, \Omega)$, then $\tilde{\nabla} \times \vec{u} \in H(\mathrm{curl}, \Omega)$. Furthermore, for homogeneous boundary conditions, if $u \in L^2(\Omega)$, then

$$\langle \tilde{\nabla} \times \tilde{\nabla} u, v \rangle_\Omega = \langle \tilde{\nabla} u, \nabla_\perp v \rangle_\Omega - \int_{\partial\Omega} v((\tilde{\nabla} u) \times \vec{n}) d\Gamma = -\langle u, \nabla \cdot \nabla_\perp v \rangle_\Omega + \int_{\partial\Omega} u(\nabla_\perp v \cdot \hat{n}) d\Gamma - \int_{\partial\Omega} v((\tilde{\nabla} u) \times \vec{n}) d\Gamma = 0.$$

For a proof of this relationship with non-homogeneous boundary conditions see [7, p. 546]. Therefore these weak operator also form an exact sequence

$$0 \leftarrow H(\mathrm{curl}, \Omega) \xleftarrow{\tilde{\nabla} \times} H(\mathrm{div}, \Omega) \xleftarrow{\tilde{\nabla}} L^2(\Omega) \leftarrow \mathbb{R}. \tag{2.25}$$

Similarly, if $u \in L^2(\Omega)$, by definition, $\nabla_\perp u \in H(\mathrm{rot}, \Omega)$. And if $u \in H(\mathrm{rot}, \Omega)$, then $\tilde{\nabla} \cdot u \in H^1(\Omega)$. Furthermore, if $u \in L^2(\Omega)$, then

$$\langle \widetilde{\nabla} \cdot \widetilde{\nabla_\perp} u, v \rangle_\Omega = -\langle \widetilde{\nabla_\perp} u, \nabla v \rangle + \int_{\partial\Omega} v(\widetilde{\nabla_\perp} u \cdot \vec{n}) d\Gamma = -\langle u, \nabla \times \nabla v \rangle - \int_{\partial\Omega} u(\nabla v \times \vec{n}) d\Gamma + \int_{\partial\Omega} v(\widetilde{\nabla_\perp} u \cdot \vec{n}) d\Gamma = 0$$

for homogeneous boundary conditions. Which means that these spaces form this last exact sequence

$$0 \leftarrow H^1(\Omega) \xleftarrow{\tilde{\nabla} \cdot} H(\mathrm{rot}, \Omega) \xleftarrow{\tilde{\nabla}_\perp} L^2(\Omega) \leftarrow \mathbb{R}. \tag{2.26}$$

These exact sequences give us a way to choose the solution and trial spaces to solve based on a given boundary value problem. This process is explained in the next subsection, using the already introduced steady heat equation.

2.3.1. The mixed form steady heat equation

As seen before (2.16), we look at the steady heat equation with $\kappa = 1$

$$\begin{aligned} &\text{find } u \in U \text{ such that} \\ &\begin{cases} -\nabla \cdot \nabla u = f, & \text{in } \Omega, \\ u = g_E, & \text{on } \Gamma_E, \\ \nabla u \cdot \vec{n} = g_N, & \text{on } \Gamma_N. \end{cases} \end{aligned} \tag{2.27}$$

To further illustrate the usage of these complexes and to introduce the *mixed form* formulation, we first rewrite this equation as a system of first order differential equations.

$$\begin{aligned} &\text{find } u \in U_u \text{ and } \vec{q} \in U_q \text{ such that} \\ &\begin{cases} -\nabla u = \vec{q}, & \text{in } \Omega, \\ \nabla \cdot \vec{q} = f, & \text{in } \Omega, \\ u = g_E, & \text{on } \Gamma_E, \\ \nabla u \cdot \vec{n} = -\vec{q} \cdot \vec{n} = g_N, & \text{on } \Gamma_N, \end{cases} \end{aligned} \tag{2.28}$$

where now we have $u \in U_u = C^2(\Omega)$ and $\vec{q} \in U_q = \left[C^1(\Omega)\right]^2$.

We follow a similar approach as discussed before, and write these equations in weak form

$$\begin{aligned} &\text{Find } u \in U_u^w \text{ and } \vec{q} \in U_q^w \text{ such that} \\ &\begin{cases} -\langle \nabla u, \vec{v}_1 \rangle_\Omega = \langle \vec{q}, \vec{v}_1 \rangle_\Omega, & \forall \vec{v}_1 \in V_q^w, \\ \langle \nabla \cdot \vec{q}, v_2 \rangle_\Omega = f, & \forall v_2 \in V_u^w, \\ u = g_E, & \text{on } \Gamma_E, \\ \nabla u \cdot n = \vec{q} \cdot \vec{n} = g_N, & \text{on } \Gamma_N. \end{cases} \end{aligned} \tag{2.29}$$

First note that, since $\vec{q}$ is a vector, $\vec{q}$ is either in $H(\mathrm{div}, \Omega)$ or in $H(\mathrm{rot}, \Omega)$. While u, since it is a scalar, is either in $L^2(\Omega)$ or $H^1(\Omega)$ (which is isomorphic to $H(\mathrm{curl}, \Omega)$ in 2D). Further, we need to compute the divergence of $\vec{q}$ and

the gradient of u. Both operations (divergence and gradient) can act either strongly or weakly, but not both at the same time (otherwise we would required the intersection of spaces, which is complicated, especially so at the discrete level). This gives us two different options, the first is equivalent to the primal form we discussed before (2.19) and the second one is a new formulation, called the *mixed form*.

The first formulation is

$$\begin{aligned} &\text{Find } u \in \widetilde{U}_{u,E} \text{ and } \vec{q} \in \widetilde{U}_q \text{ such that} \\ &\begin{cases} \langle \nabla u, \vec{v}_1 \rangle_\Omega = \langle \vec{q}, \vec{v}_1 \rangle_\Omega \,, & \forall \vec{v}_1 \in \widetilde{V}_q \\ -\langle \vec{q}, \nabla v_2 \rangle_\Omega + \displaystyle\int_{\Gamma_N} v_2 \underbrace{g_N}_{\vec{q}\cdot\vec{n}|_{\Gamma_N}} \mathrm{d}\Gamma_N = \langle f, v_2 \rangle_\Omega \,, & \forall v_2 \in \widetilde{V}_{u,0} \,, \end{cases} \end{aligned} \tag{2.30}$$

where

$$\widetilde{U}_{u,E} := \left\{ u \in \widetilde{U}_u = H^1(\Omega) : \, u|_{\Gamma_E} = g_E \right\}, \tag{2.31}$$

$$\widetilde{V}_{u,0} := \left\{ v \in \widetilde{V}_u = H^1(\Omega) : \, v|_{\Gamma_E} = 0 \right\}, \tag{2.32}$$

and $\widetilde{U}_q = \widetilde{V}_q = H(\mathrm{rot}, \Omega)$. As seen before, these equations can be expressed in compact notation as

$$\begin{aligned} &\text{Find } u \in \widetilde{U}_{u,E} \text{ and } \vec{q} \in \widetilde{U}_q \text{ such that} \\ &\begin{cases} \langle \nabla u, \vec{v}_1 \rangle_\Omega = \langle \vec{q}, \vec{v}_1 \rangle_\Omega \,, & \forall \vec{v}_1 \in \widetilde{V}_q \\ \langle \widetilde{\nabla} \cdot \vec{q}, v_2 \rangle_\Omega = \langle f, v_2 \rangle_\Omega \,, & \forall v_2 \in \widetilde{V}_{u,0} \,. \end{cases} \end{aligned} \tag{2.33}$$

The second formulation, the so called *mixed form*, is

$$\begin{aligned} &\text{Find } u \in \widetilde{U}_u \text{ and } \vec{q} \in \widetilde{U}_{q,N} \text{ such that} \\ &\begin{cases} \langle u, \nabla \cdot \vec{v}_1 \rangle - \displaystyle\int_{\Gamma_E} \underbrace{g_E}_{u|_{\Gamma_E}} \vec{v}_1 \cdot \vec{n} \, \mathrm{d}\Gamma_E = \langle \vec{q}, \vec{v}_1 \rangle \,, & \forall \vec{v}_1 \in \widetilde{V}_{q,0} \\ \langle \nabla \cdot \vec{q}, v_2 \rangle = \langle f, v_w \rangle \,, & \forall v_2 \in \widetilde{V}_u \,, \end{cases} \end{aligned} \tag{2.34}$$

where

$$\widetilde{U}_{q,N} := \left\{ \vec{q} \in \widetilde{U}_q = H(\mathrm{div}, \Omega) : \, \vec{q} \cdot \vec{n}\big|_{\Gamma_N} = g_N \right\}, \tag{2.35}$$

$$\widetilde{V}_{q,0} := \left\{ \vec{v} \in \widetilde{V}_q = H(\mathrm{div}, \Omega) : \, \vec{v}|_{\Gamma_N} = 0 \right\}, \tag{2.36}$$

and $\widetilde{U}_u = \widetilde{V}_u = L^2(\Omega)$. As seen before, these equations can be expressed in compact notation as

$$\begin{aligned} &\text{Find } u \in \widetilde{U}_u \text{ and } \vec{q} \in \widetilde{U}_{q,N} \text{ such that} \\ &\begin{cases} \langle \widetilde{\nabla} u, \vec{v}_1 \rangle_\Omega = \langle \vec{q}, \vec{v}_1 \rangle_\Omega \,, & \forall \vec{v}_1 \in \widetilde{V}_{q,0} \\ \langle \nabla \cdot \vec{q}, v_2 \rangle_\Omega = \langle f, v_2 \rangle_\Omega \,, & \forall v_2 \in \widetilde{V}_u \,. \end{cases} \end{aligned} \tag{2.37}$$

Note that, in any of the two formulations, only one of the two differential operators acts strongly and therefore only one of the equations is exactly satisfied. If the first system is chosen, this means that means that $\nabla p = \vec{u}$ is exactly (strongly) satisfied and by substituting this into the system of equations we get exactly the same equation as (2.19). We will discuss what these two situations mean for the boundary conditions in the next section.

2.4. Finite element method

In the previous sections we have introduced for a general boundary value problem its *strong* (2.1) and *weak* (2.2) forms and used the steady heat equation to present concrete examples of the strong form, (2.16), and weak form, (2.19). Additionally we have introduced the *mixed form* (2.34). Also we have introduced the weak differential operators $\widetilde{\nabla}$ (2.11), $\widetilde{\nabla}\cdot$ (2.12), $\widetilde{\nabla}\times$ (2.13) and $\widetilde{\nabla}_\perp$ (2.14), together with the weak function spaces that guarantee that our equations in weak form are meaningful, (2.7). Additionally, we introduced and discussed the De Rham complex and highlighted its importance.

The key idea of the finite element method is to setup a discrete version of the weak form of a boundary value problem (e.g. (2.15), (2.19), or (2.34)). In order to do so, it is fundamental to construct discrete function

spaces which, as a refinement parameter is increased, allows us to improve the approximation. Now, let us consider the weak form for the general problem we discussed before (2.15),

$$\begin{aligned} &\text{find } u \in \widetilde{U} \text{ such that} \\ \langle \widetilde{\mathscr{L}}[u], v\rangle_\Omega = 0\,, \qquad &\forall v \in \widetilde{V}\,, \qquad (2.38)\\ u = g_E\,, \text{ on } \Gamma_E\,, \qquad &(2.39)\\ \mathscr{D}[u] = g_N\,, \text{ on } \Gamma_N\,, \qquad &(2.40) \end{aligned}$$

where $u \in \widetilde{U}$.

As we saw before, for the concrete case of the steady heat equation (2.22), we can rewrite (2.41) as

$$\begin{cases} \text{Find } u \in \widetilde{U}_E \text{ such that} \\ \langle \widetilde{\mathscr{L}}[u], v\rangle_\Omega = 0\,, \qquad \forall v \in \widetilde{V}_0\,, \end{cases} \tag{2.41}$$

where

$$\widetilde{U}_E = \left\{ u \in \widetilde{U} : u|_{\Gamma_E} = g_E \right\}, \tag{2.42}$$

$$\widetilde{V}_0 = \left\{ v \in \widetilde{V} : v|_{\Gamma_E} = 0 \right\}, \tag{2.43}$$

as done before. Also note that, as before, we have included the natural boundary conditions (over Γ_N), into the weak differential operator $\widetilde{\mathscr{L}}$.

The (discrete) finite element formulation of this problem corresponds to

$$\begin{cases} \text{Find } u_E^h \in \widetilde{U}_E^h \text{ such that} \\ \langle \widetilde{\mathscr{L}}[u^h], v^h\rangle_\Omega = 0\,, \qquad \forall v^h \in \widetilde{V}_0^h\,, \end{cases} \tag{2.44}$$

with

$$\widetilde{U}_E^h = \left\{ u^h \in \widetilde{U}^h : u^h\Big|_{\Gamma_E} = g_E^h \right\}, \tag{2.45}$$

$$\widetilde{V}_0^h = \left\{ v^h \in \widetilde{V}^h : v^h\Big|_{\Gamma_E} = 0 \right\}, \tag{2.46}$$

where

$$\widetilde{U}^h \subset \widetilde{U}, \qquad \widetilde{V}^h \subset \widetilde{V}\,, \tag{2.47}$$

are discrete (finite dimensional) subsets, and h is the refinement parameter (e.g. a mesh size, or polynomial degree). Note that, since the spaces are discrete, we can easily express them as the span of a finite dimensional basis, N_i, with $i = 1, \ldots, n_{\widetilde{U}}$, i.e.,

$$\widetilde{U}^h = \text{span}\,\{N_i\}_{i=1}^{n_{\widetilde{U}}}\,. \tag{2.48}$$

As a consequence, we can express any function of these finite dimensional spaces, including the (approximate) solution, $u^h \in \widetilde{U}^h$, as a linear combination of the basis functions

$$u^h = \sum_{i=1}^{n_{\widetilde{U}}} u_i N_i\,. \tag{2.49}$$

For the case $u_E^h \in \widetilde{U}_E^h$ we need to separate the part that influences the values at the boundary Γ_E and the remaining of the domain

$$u_E^h = \sum_{i=1}^{n_{\widetilde{U}_E}} u_i N_i + g_E^h\,, \tag{2.50}$$

where g_E^h approximates the boundary conditions over Γ_E and the other term, $\sum_{i=1}^{n_{\widetilde{U}_E}} u_i N_i$, is zero at Γ_E, in order not to perturb the boundary conditions.

The finite element method is obtained by substituting (2.50) into (2.44) and using the basis N_i instead of v_h as test functions

$$\begin{aligned} &\text{Find } u_E^h \in \widetilde{U}_E^h \text{ such that} \\ \langle \widetilde{\mathscr{L}}[\sum_{i=1}^{n_{\widetilde{U}_E}} u_i N_i + g_E^h], N_j\rangle_\Omega = 0\,, &j = 1, \ldots, n_{\widetilde{U}_E}\,. \qquad (2.51) \end{aligned}$$

Note that the equation only needs to be satisfied for the basis functions of $\widetilde{V}^h$, since equation (2.44) is linear with regards to the test functions and the test functions can be expressed as a linear combination of the basis functions of the finite space. This means that the equation hols for all the basis functions, it holds for all functions in $\widetilde{V}^h$.
If the operator $\widetilde{\mathscr{L}}$ is linear we can expand this expression as

$$\text{Find } u_E^h \in \widetilde{U}_E^h \text{ such that}$$
$$\sum_{i=1}^{n_{\widetilde{U}_E}} u_i \langle \widetilde{\mathscr{L}}[N_i], N_j \rangle_\Omega = -\langle \widetilde{\mathscr{L}}[g_E^h], N_j \rangle_\Omega, j = 1, \ldots, n_{\widetilde{U}_E}. \tag{2.52}$$

Now we will first introduce and discuss the discrete function spaces we will use in this work and then setup the finite element formulation for both the primal (2.22), and mixed form (2.37) of the steady heat equation (2.16).

2.4.1. Discrete de Rham complex

We choose our discrete spaces in such a way that they mirror the de Rham complexes as described in section 2.3. We pick discrete spaces $W_h \subset H(\text{curl}, \Omega)$, $V_h \subset H(\text{div}, \Omega)$, $Q_h \subset L^2(\Omega)$, $R_h \subset H^1(\Omega)$ and $K_h \subset H(\text{rot}, \Omega)$. This way the relations between the spaces $H(\text{curl}, \Omega)$, $H(\text{div}, \Omega)$, $L^2(\Omega)$, $H^1(\Omega)$ and $H(\text{rot}, \Omega)$ also hold for the discrete spaces W_h, V_h, Q_h, R_h and K_h.

$$\mathbb{R} \to W_h \xrightarrow{\nabla_\perp} V_h \xrightarrow{\nabla \cdot} Q_h \to 0 \tag{2.53}$$
$$0 \leftarrow W_h \xleftarrow{\tilde{\nabla} \times} V_h \xleftarrow{\tilde{\nabla}} Q_h \leftarrow \mathbb{R} \tag{2.54}$$
$$\mathbb{R} \to R_h \xrightarrow{\nabla} K_h \xrightarrow{\nabla \times} Q_h \to 0 \tag{2.55}$$
$$0 \leftarrow R_h \xleftarrow{\tilde{\nabla} \cdot} K_h \xleftarrow{\tilde{\nabla}_\perp} Q_h \leftarrow \mathbb{R} \tag{2.56}$$

We now choose a set of basis functions that are zero that are equal to zero every in the domain, except for some closed subset of the domain. These basis functions are called *elements*. What this closed subset is depends on how the domain is split into smaller parts. This partition of the domain is called the *mesh*. In this report W_h and R_h are the continuous Lagrange elements [12, p. 94,95] of degree p, these elements are made up polynomial functions of degree p of both the x and y spatial variable. V_h and K_h are the Raviart-Thomas elements [12, p. 98] of degree p, which are made up of vector functions, where the x-component is a polynomial of order p of the x variable and of order $(p-1)$ of the y variable and the y-component is a polynomial of order $(p-1)$ of the x variable and order p of the y variable. Q_h are the discontinuous Lagrange elements [12, p. 105] of degree $(p-1)$, which are polynomials of order $p-1$ of the x and y variables. These elements have been shown to satisfy the properties to form these exact sequences [1]. For a further discussion of these elements see [12].
In this report we will use a triangular mesh for the Navier-Stokes equations, made up of squares separated into two triangles by an edge from the top left to the bottom right of the square. A 2×2 example of such a mesh can be seen in figure 2.1a. In figure 2.1b an example of a 1st order continuous Lagrange element on this mesh is shown. In figure 2.1c a 1st order Raviart-Thomas element is shown and in figure 2.1d a 0th order discontinuous Lagrange element is shown.

2.4.2. The discrete primal form steady heat equation

The weak form of the steady heat equation (2.19) is our starting point

$$\text{Find } u_E \in \widetilde{U}_E, \text{ such that}$$
$$\langle \nabla u, \nabla v \rangle_\Omega - \int_{\Gamma_N} g_N v \, \mathrm{d}\Gamma_N = \langle f, v \rangle_\Omega, \forall v \in \widetilde{V}_0, \tag{2.57}$$

where

$$\widetilde{U}_E := \left\{ u \in \widetilde{U} = H^1(\Omega) : \; u|_{\Gamma_E} = g_E \right\}, \tag{2.58}$$

and

$$\widetilde{V}_0 := \left\{ v \in \widetilde{V} = H^1(\Omega) : \; v|_{\Gamma_E} = 0 \right\}. \tag{2.59}$$

As discussed before, in the finite element method we rewrite this weak form as a discrete weak form using discrete spaces. We have already introduced the discrete function spaces, see section 2.4.1, therefore we can

just make the substitution $H^1(\Omega) \to W_h$, which enables us to construct $\widetilde{U}^h$ and $\widetilde{V}^h$ and, consequently, $\widetilde{U}_E^h$ and $\widetilde{V}_0^h$. We can then write down the discrete weak form

$$\begin{aligned} &\text{Find } u_E^h \in \widetilde{U}_E^h, \text{ such that} \\ &\langle \nabla u^h, \nabla v^h \rangle_\Omega - \int_{\Gamma_N} g_N^h v^h \, \mathrm{d}\Gamma_N = \langle f, v^h \rangle_\Omega, \forall\, v^h \in \widetilde{V}_0 \,. \end{aligned} \tag{2.60}$$

If we now substitute v^h by each of the basis functions in $\widetilde{U}_E$ and u^h by its expansion $u^h = \sum_{i=1}^{n_{\widetilde{U}_E}} u_i N_i + g_E^h$, we get

$$\begin{aligned} &\text{Find } u^h = \sum_{i=1}^{n_{\widetilde{U}_E}} u_i N_i + g_E^h \in \widetilde{U}_E^h, \text{ such that} \\ &\sum_{i=1}^{n_{\widetilde{U}_E}} u_i \underbrace{\langle \nabla N_i, \nabla N_j \rangle_\Omega}_{\mathbf{S}_{ij}} + \underbrace{\langle \nabla g_E^h, \nabla N_j \rangle_\Omega}_{\mathbf{b}_{E,j}} - \underbrace{\int_{\Gamma_N} g_N^h N_j \, \mathrm{d}\Gamma_N}_{\mathbf{b}_{N,j}} = \underbrace{\langle f, N_j \rangle_\Omega}_{\mathbf{f}_j}, \qquad j = 1, \ldots, n_{\widetilde{U}_E} \,. \end{aligned} \tag{2.61}$$

We can then rewrite this expression in a compact matrix form,

$$\begin{aligned} &\text{Find } \mathbf{u} = \begin{bmatrix} u_1 \\ u_2 \\ \cdots \\ u_{n_{\widetilde{U}_E}} \end{bmatrix} \in \operatorname{span}\{N_i\}_{i=1}^{n_{\widetilde{U}_E}} \text{ such that} \\ &\mathbf{S}\mathbf{u} = \mathbf{f} + \mathbf{b}_N - \mathbf{b}_E \,. \end{aligned}$$

2.4.3. The discrete mixed form steady heat equation

Now the weak form of the mixed form heat equation, (2.34), is our starting point.

$$\begin{cases} \text{Find } u \in \widetilde{U}_u \text{ and } \vec{q} \in \widetilde{U}_{q,N} \text{ such that} \\ \langle u, \nabla \cdot \vec{v}_1 \rangle - \displaystyle\int_{\Gamma_E} g_E \vec{v}_1 \cdot \vec{n} \, \mathrm{d}\Gamma_E = \langle \vec{q}, \vec{v}_1 \rangle \,, & \forall\, \vec{v}_1 \in \widetilde{V}_{q,0} \\ \langle \nabla \cdot \vec{q}, v_2 \rangle = \langle f, v_2 \rangle \,, & \forall\, v_2 \in \widetilde{V}_u \,, \end{cases}$$

where

$$\widetilde{U}_{q,N} := \left\{ \vec{q} \in \widetilde{U}_q = H(\mathrm{div}, \Omega) : \ \vec{q} \cdot \vec{n}\big|_{\Gamma_N} = g_N \right\},$$

$$\widetilde{V}_{q,0} := \left\{ \vec{v} \in \widetilde{V}_q = H(\mathrm{div}, \Omega) : \ \vec{v}|_{\Gamma_N} = 0 \right\},$$

and $\widetilde{U}_u = \widetilde{V}_u = L^2(\Omega)$. As before we substitute the continuous function spaces for their discrete counterparts. $H(\mathrm{div}, \Omega) \to V_h$ and $L^2(\Omega) \to Q_h$, which allows us to construct $\widetilde{U}_u^h$, $\widetilde{V}_u^h$, $\widetilde{U}_q^h$ and $\widetilde{V}_q^h$. Consequently we can construct $\widetilde{U}_{q,N}^h$ and $\widetilde{V}_{q,0}$, note that this step is not necessary for the spaces for u, since there are no essential boundary conditions prescribed to u. This allows us to write down the discrete weak form.

$$\begin{cases} \text{Find } u^h \in \widetilde{U^h} \text{ and } \vec{q}^h \in \widetilde{U}_{q,N}^h \text{ such that} \\ \langle u^h, \nabla \cdot \vec{v}_1^h \rangle_\Omega - \displaystyle\int_{\Gamma_E} g_E \vec{v}_1^h \cdot \vec{n} \, \mathrm{d}\Gamma_E = \langle \vec{q}^h, \vec{v}_1^h \rangle_\Omega \,, & \forall\, \vec{v}_1^h \in \widetilde{V}_{q,0}^h \\ \langle \nabla \cdot \vec{q}^h, v_2^h \rangle_\Omega = \langle f, v_2 \rangle_\Omega \,, & \forall\, v_2^h \in \widetilde{V}_u^h \,, \end{cases}$$

For $\vec{q}^h \in \widetilde{U}_{q,N}^h$ we substitute $\vec{q}^h = \sum_{i=1}^{n_{\widetilde{U}_{q,N}}} q_i \vec{M}_i + g_N^h$ and for u^h we substitute $u^h = \sum_{i=1}^{n_{\widetilde{U}_u}} u_i N_i$, where g_N^h approximates the boundary condition for p over Γ_N, $\{\vec{M}_i\}_{i=1}^{n_{\widetilde{U}_u}}$ are the remaining basis functions of $\widetilde{U}_{q,N}$ and $\{N_i\}_{i=1}^{n_{\widetilde{U}_u}}$

are the basis functions of $\widetilde{U}_u$. This results in

$$\text{Find } u^h = \sum_{i=1}^{n_{\widetilde{U}_u}} u_i N_i \in \widetilde{U}_u \text{ and } \vec{q}^h = \sum_{i=1}^{n_{\widetilde{U}_{q,N}}} q_i \vec{M}_i + g_N^h \in \widetilde{U}_{q,N} \text{ such that}$$

$$\begin{cases} \sum_{i=1}^{n_{\widetilde{U}_u}} u_i \underbrace{\langle N_i, \nabla \cdot \vec{M}_j \rangle_\Omega}_{\boldsymbol{A_{ij}}} - \underbrace{\int_{\Gamma_E} g_E \vec{M}_j \cdot \vec{n} \, \mathrm{d}\Gamma_E}_{\boldsymbol{b_{E,j}}} = \sum_{i=1}^{n_{\widetilde{U}_{q,N}}} q_i \underbrace{\langle \vec{M}_i, \vec{M}_j \rangle_\Omega}_{\boldsymbol{M_{ij}}} + \underbrace{\langle g_N^h, \vec{M}_j \rangle_\Omega}_{\boldsymbol{b_{N,j}}}, & j = 1, \ldots, n_{\widetilde{U}_{q,N}}, \\ \sum_{i=1}^{n_{\widetilde{U}_{q,N}}} q_i \underbrace{\langle \nabla \cdot \vec{M}_i, N_j \rangle_\Omega}_{\boldsymbol{B_{ij}}} + \underbrace{\langle \nabla \cdot \vec{g}_N^h, N_j \rangle_\Omega}_{\boldsymbol{c_j}} = \underbrace{\langle f, N_j \rangle_\Omega}_{\boldsymbol{f_j}}, & j = 1, \ldots \widetilde{U}_u \, . \end{cases} \tag{2.62}$$

Where we have again used the fact that if these equations hold for all the basis functions, then they hold for all functions in $\widetilde{V}_{q,0}^h$ and $\widetilde{V}_u^h$.
Which we can again compactly write in matrix form,

$$\text{Find } \mathbf{q} \in \text{span}\{M_i\}_{i=1}^{n_{\widetilde{U}_{q,N}}} \text{ and } \mathbf{u} \in \text{span}\{M_i\}_{i=1}^{n_{\widetilde{U}_u}} \text{ such that}$$

$$\begin{cases} \boldsymbol{Au} - \boldsymbol{b_E} = \boldsymbol{Mq} + \boldsymbol{b_N} \\ \boldsymbol{Bq} + \boldsymbol{c} = \boldsymbol{f}. \end{cases} \tag{2.63}$$

Or equivalently,

$$\text{Find } \begin{bmatrix} \boldsymbol{q} \\ \boldsymbol{u} \end{bmatrix} \in \text{span}\{M_i\}_{i=1}^{n_{\widetilde{U}_{q,N}}} \times \text{span}\{M_i\}_{i=1}^{n_{\widetilde{U}_u}} \text{such that}$$

$$\begin{bmatrix} -\boldsymbol{M} & \boldsymbol{A} \\ \boldsymbol{B} & \boldsymbol{0} \end{bmatrix} \begin{bmatrix} \boldsymbol{q} \\ \boldsymbol{u} \end{bmatrix} = \begin{bmatrix} \boldsymbol{b_E} + \boldsymbol{b_N} \\ \boldsymbol{c_N} + \boldsymbol{f} \end{bmatrix}. \tag{2.64}$$

Where the matrices and vectors from the equations before should now be seen as submatrices and subvectors.

2.5. Finite element method for transient problems: the unsteady heat equation

As a last building block to the navier stokes equation we explain how to work out transient problem, again by working out the primal and mixed heat equations. The transient heat equation is given by:

$$\begin{cases} -\nabla^2 u = \dfrac{\partial u}{\partial t} \\ u = g_E, \text{ on } \Gamma_E \\ \nabla u \cdot \hat{n} = G_N, \text{ on } \Gamma_N. \end{cases} \tag{2.65}$$

Where now we have u needs to be twice continuous differentiable in space and once in time.

2.5.1. Primal form unsteady heat equation

All the steps for the transient problem are completely analogous to those in section 2.4.2, with $f = \frac{\partial u}{\partial t}$. Therefore we take equation 2.61 as starting point and substitute $\frac{\partial u^h}{\partial t}$ for f.

$$\text{Find } u^h = \sum_{i=1}^{n_{\widetilde{U}_E}} u_i N_i + g_E^h \in \widetilde{U}_E^h, \text{ such that}$$

$$\sum_{i=1}^{n_{\widetilde{U}_E}} u_i \langle \nabla N_i, \nabla N_j \rangle_\Omega + \langle \nabla g_E^h, \nabla N_j \rangle_\Omega - \int_{\Gamma_N} g_N^h N_j \, \mathrm{d}\Gamma_N = \langle \frac{\partial u^h}{\partial t}, N_j \rangle_\Omega, \qquad j = 1, \ldots, n_{\widetilde{U}_E}.$$

Now substituting $u^h = \sum_{i=1}^{n_{\tilde{U}_E}} u_i N_i + g_E^h$ into the equation results in

$$\text{Find } u^h = \sum_{i=1}^{n_{\tilde{U}_E}} u_i N_i + g_E^h \in \widetilde{U}_E^h, \text{ such that}$$

$$\sum_{i=1}^{n_{\tilde{U}_E}} u_i \langle \nabla N_i, \nabla N_j \rangle_\Omega + \langle \nabla g_E^h, \nabla N_j \rangle_\Omega - \int_{\Gamma_N} g_N^h N_j \, \mathrm{d}\Gamma_N = \sum_{i=1}^{n_{\tilde{U}_E}} \frac{du_i}{dt} \langle N_i, N_j \rangle_\Omega + \langle \frac{\partial g_E^h}{\partial t}, N_j \rangle_\Omega, \qquad j = 1, \ldots, n_{\tilde{U}_E}. \tag{2.66}$$

Here the basis functions,N_i are a function of only space and the combination scalars u_i are functions of only time, therefore the partial derivative changes to a full derivative.
Using the midpoint method and the midpoint rule to evaluate the time derivative yields.

$$\sum_{i=1}^{n_{\tilde{U}_E}} \frac{u_i^{k+1} + u_i^k}{2} \underbrace{\langle \nabla N_i, \nabla N_j \rangle_\Omega}_{\boldsymbol{S_{ij}}} + \underbrace{\langle \nabla g_E^h, \nabla N_j \rangle_\Omega}_{\boldsymbol{b_{E,j}}} - \underbrace{\int_{\Gamma_N} g_N^h N_j \, \mathrm{d}\Gamma_N}_{\boldsymbol{b_{N,j}}} = \sum_{i=1}^{n_{\tilde{U}_E}} \frac{u_i^{k+1} - u_i^k}{\Delta t} \underbrace{\langle N_i, N_j \rangle_\Omega}_{\boldsymbol{N_{ij}}} + \underbrace{\langle \frac{(g_E^h)^{k+1} - (g_E^h)^k}{\Delta t}, N_j \rangle_\Omega}_{\boldsymbol{g_j}}, \qquad j = 1, \ldots, n_{\tilde{U}_E}$$

Where Δt is our chosen time step, u_i^k is u_i evaluated at time $(k\Delta t)$. We can also write this in the compact vector notation.

$$\frac{1}{2}\boldsymbol{S}\boldsymbol{u}^{\boldsymbol{k+1}} + \frac{1}{2}\boldsymbol{S}\boldsymbol{u}^{\boldsymbol{k}} + \boldsymbol{b_E} - \boldsymbol{b_N} = \frac{1}{\Delta t}\boldsymbol{N}\boldsymbol{u}^{\boldsymbol{k+1}} - \frac{1}{\Delta t}\boldsymbol{N}\boldsymbol{u}^{\boldsymbol{k}} + \boldsymbol{g_j} \tag{2.67}$$

Where $\boldsymbol{u^k} = [u_1^k, u_2^k, \ldots u_{n_{\widetilde{U}_E}}^k]$. Thus given $\boldsymbol{u^0}$ we can calculate $\boldsymbol{u^1}$ and through iteration any $\boldsymbol{u^k}$.

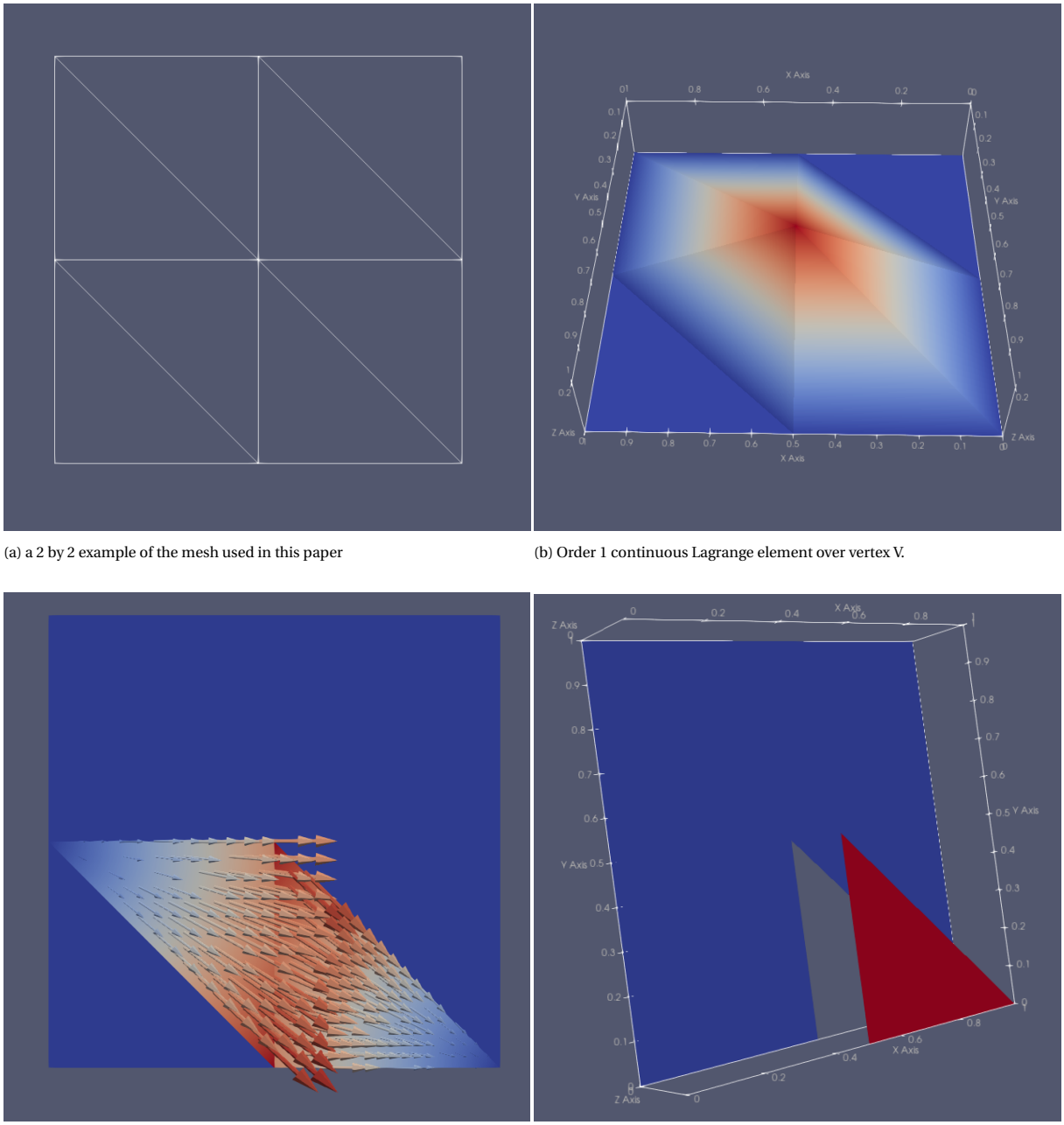

(a) a 2 by 2 example of the mesh used in this paper

(b) Order 1 continuous Lagrange element over vertex V.

(c) Order 1 Raviart-Thomas element over the edge E.

(d) Order 0 discontinuous Lagrange element over the plane P

Figure 2.1: Figure showing an example of the type of mesh and the three types of basis functions used in this paper.

3

A mass, energy, vorticity and enstrophy conservative discretization for the Navier-Stokes equation

3.1. Strong form

The Navier-Stokes equation is an equation which describes the movement of viscous fluids. We will look specifically at the dimensionless, 2D, incompressible Navier-Stockes equations in the rotational form [19]:

$$\frac{\partial \vec{u}}{\partial t} + \omega \times \vec{u} + \mathrm{Re}^{-1}\nabla_{\perp}\omega + \nabla P = \vec{f}, \text{ in } \Omega \times (0,T] \tag{3.1}$$

$$\omega - \nabla \times \vec{u} = 0, \text{ in } \Omega \times (0,T] \tag{3.2}$$

$$\nabla \cdot \vec{u} = 0, \text{ in } \Omega \times (0,T] \tag{3.3}$$

$$\vec{u} \cdot \hat{n} = u_{\perp}, \text{ on } \Gamma \times (0,T] \tag{3.4}$$

$$\vec{u} \times \hat{n} = u_{\parallel}, \text{ on } \Gamma \times (0,T]. \tag{3.5}$$

Where $\vec{u}$ is the velocity, ω is the vorticity, $P := p + \frac{1}{2}\vec{u}\cdot\vec{u}$ is the total pressure, with p the static pressure, $\vec{f}$ is the total body force and $a \times \vec{b} = -ab_y\vec{e}_x + ab_x\vec{e}_y$.

3.2. Conservation properties

The incompressible Navier-Stokes equations as given in (3.1-3.5) has the following conservation properties.

3.2.1. mass conservation

Since we assume no mass is being created, the change of mass inside the boundary can be described completely by the flow over the boundary.

$$\frac{\partial M}{\partial t} + \int_{\partial\Omega} \rho \vec{u} \cdot \vec{n} d\Gamma = 0 \tag{3.6}$$

Where M is the total mass inside the boundary, ρ is the density and $\vec{n}$ is the outward pointing unit normal vector. Then, by the divergence theorem[cite it],

$$\frac{\partial M}{\partial t} + \int_{\Omega} \nabla \cdot (\rho \vec{u}) d\Omega = 0. \tag{3.7}$$

Since we are looking at the incompressible Navier-Stokes, ρ will be constant in space.

$$\frac{\partial M}{\partial t} + \rho \int_{\Omega} \nabla \cdot \vec{u} d\Omega = 0. \tag{3.8}$$

Using equation (3.3), this means mass is conserved.

3.2.2. Kinetic energy

The kinetic energy in the fluid in dimensionless form is given by the equation,

$$K = \frac{1}{2}\int_\Omega \vec{u}\cdot\vec{u}d\Omega. \tag{3.9}$$

Therefor the time derivative is,

$$\frac{dK}{dt} = \frac{d}{dt}\frac{1}{2}\int_\Omega \vec{u}\cdot\vec{u}d\Omega = \int_\Omega \frac{\partial\vec{u}}{\partial t}\cdot\vec{u}d\Omega = \langle\frac{\partial\vec{u}}{\partial t},\vec{u}\rangle_\Omega \tag{3.10}$$

Where the full derivative becomes a partial derivative, because $\vec{u}$ is a function of space, while $\int_\Omega \vec{u}\cdot\vec{u}d\Omega$ is not. If take the dot product of equation (3.1) and integrate over Ω we get,

$$\langle\frac{\partial\vec{u}}{\partial t},\vec{u}\rangle_\Omega + \langle\omega\times\vec{u},\vec{u}\rangle_\Omega + \mathrm{Re}^{-1}\langle\nabla_\perp\omega,\vec{u}\rangle_\Omega + \langle\nabla P,\vec{u}\rangle_\Omega = \langle\vec{f},\vec{u}\rangle_\Omega. \tag{3.11}$$

Here the first term is equal to $\frac{\partial K}{\partial t}$ and therefor,

$$\frac{dK}{dt} = -\langle\omega\times\vec{u},\vec{u}\rangle_\Omega - \mathrm{Re}^{-1}\langle\nabla_\perp\omega,\vec{u}\rangle_\Omega - \langle\nabla P,\vec{u}\rangle_\Omega + \langle\vec{f},\vec{u}\rangle_\Omega \tag{3.12}$$

We will analyse this equation term by term. The first term is 0, since $\omega\times\vec{u}\perp\vec{u}$. Applying integration by parts on the second term results in,

$$\langle\nabla_\perp\omega,\vec{u}\rangle_\Omega = \langle\omega,\nabla\times\vec{u}\rangle_\Omega + \int_{\partial\Omega}\omega(\vec{u}\times\vec{n})d\Gamma = \langle\omega,\omega\rangle_\Omega + \int_{\partial\Omega}\omega(\vec{u}\times\vec{n})d\Gamma \tag{3.13}$$

Since, by equation (3.3), $\nabla\times\vec{u}=\omega$. Similarly, integration by parts on the third term results in,

$$\langle\nabla P,\vec{u}\rangle_\Omega = -\langle P,\nabla\cdot\vec{u}\rangle_\Omega + \int_{\partial\Omega}P\vec{u}\cdot\vec{n}d\Gamma = \int_{\partial\Omega}P\vec{u}\cdot\vec{n}d\Gamma \tag{3.14}$$

Since $\nabla\cdot\vec{u}=0$. Putting all of this together results in,

$$\frac{dK}{dt} = -\mathrm{Re}^{-1}\langle\omega,\omega\rangle_\Omega - \mathrm{Re}^{-1}\int_{\partial\Omega}\omega u_\parallel d\Gamma - \int_{\partial\Omega}Pu_\perp d\Gamma + \langle\vec{f},\vec{u}\rangle_\Omega \tag{3.15}$$

Where we have used the boundary conditions (3.4-3.5). We will again analyse this result term by term. The first term is twice the total enstrophy, E. The second term will be zero if $u_\parallel=0$. The third term will be zero if $u_\perp=0$. The final term will be zero if $\vec{f}$ is conservative and $u_\perp=0$. This can be shown as follows. If $\vec{f}$ is conservative, then there exist some potential ϕ such that $\vec{f}=\nabla\phi$. Plugging this into the fourth term and using integration by parts results in,

$$\langle\nabla\phi,\vec{u}\rangle_\Omega = -\langle\phi,\nabla\cdot\vec{u}\rangle_\Omega + \int_{\partial\Omega}\phi\vec{u}\cdot\vec{n}d\Gamma = \int_{\partial\Omega}\phi u_\perp d\Gamma \tag{3.16}$$

Where we used that $\nabla\cdot\vec{u}=0$ and $\vec{u}\cdot\vec{n}=u_\perp$. Which is zero if $u_\perp=0$

3.2.3. vorticity

The equation for total vorticity is given by,

$$V = \int_\Omega \omega d\omega = \int_\Omega \nabla\times\vec{u}d\omega. \tag{3.17}$$

where equation (3.2) was used. Therefore the change of the total vorticity is given by,

$$\frac{dV}{dt} = \int_\Omega \nabla\times\frac{\partial\vec{u}}{\partial t}d\Omega. \tag{3.18}$$

By taking the curl of equation (3.1) and integrating over Ω, we see that

$$\frac{dV}{dt} = \int_\Omega \nabla\times(\omega\times\vec{u})d\Omega + \mathrm{Re}^{-1}\int_\Omega \nabla\times\nabla_\perp\omega d\Omega + \int_\Omega \nabla\times\nabla P d\Omega = \int_\Omega \nabla\times f d\Omega \tag{3.19}$$

For the first term it holds that,

$$\int_\Omega \nabla \times (\omega \times \vec{u}) d\Omega = \int_\Omega \nabla \times \begin{bmatrix} -\omega u_y \\ \omega u_x \end{bmatrix} d\Omega = \int_\Omega \frac{\partial(\omega u_x)}{\partial x} + \frac{\partial(\omega u_y)}{\partial y} d\Omega = \int_\Omega \nabla \cdot (\omega \vec{u}) d\Omega = \int_{\partial\Omega} \omega(\vec{u} \cdot \vec{n}) d\Gamma \tag{3.20}$$
$$= \int_{\partial\Omega} \omega u_\perp d\Gamma$$

Where in the first step we used that $a \times \vec{b} = -ab_y\vec{e}_x + ab_x\vec{e}_y$. In the second step the definition of the rotor, given in chapter 2.2, is used. For the third step the definition of the divergence is used. For the forth step the divergence theorem was used. This results is equal to zero, when $u_\perp = 0$. For the second term, by stokes' theorem,

$$\int_\Omega \nabla \times \nabla_\perp \omega d\Omega = \int_{\partial\Omega} \nabla_\perp \omega \cdot \vec{t} d\Gamma \tag{3.21}$$

where $\vec{t}$ is the unit vector tangent to the boundary. The third term is zero, since $\nabla \times \nabla(\cdot) = 0$. And the forth term is zero if $\vec{f}$ is conservative, since then we can again write $\vec{f} = \nabla\phi$ and therefor $\nabla \times \nabla\phi = 0$.

3.2.4. Enstrophy

For incompressible flow, the enstrophy is given by,

$$E = \frac{1}{2}\int_\Omega \omega^2 d\Omega \tag{3.22}$$

Taking the curl of equation (3.1), multiplying by ω and integrating over Ω yields,

$$\langle \nabla \times \frac{\partial \vec{u}}{\partial t}, \omega \rangle_\Omega + \langle \nabla \times (\omega \times \vec{u}), \omega \rangle_\Omega + \mathrm{Re}^{-1} \langle \nabla \times \nabla_\perp \omega, \omega \rangle_\Omega + \langle \nabla \times \nabla P, \omega \rangle_\Omega = \langle \nabla \times \vec{f}, \omega \rangle_\Omega \tag{3.23}$$

Here the first term is the total enstrophy. Using integration by parts on the second term yields,

$$\langle \nabla \times (\omega \times \vec{u}), \omega \rangle_\Omega = \langle \omega \times \vec{u}, \nabla_\perp \omega \rangle_\Omega - \int_{\partial\Omega} \omega(\omega \times \vec{u} \times \vec{n}) d\Gamma \tag{3.24}$$

Where the boundary term is zero for homogeneous boundary conditions and for the other term will be shown to be zero. Since $\nabla \cdot \vec{u}$ we are able to write $\vec{u} = \nabla_\perp \phi$, were for some ϕ. This means that we can rewrite the second equation as,

$$\langle \omega \times \vec{u}, \nabla_\perp \omega \rangle_\Omega = \langle \nabla \cdot (\omega\phi), \nabla_\perp \omega \rangle_\Omega - \langle \phi \times \nabla_\perp \omega, \nabla_\perp \omega \rangle_\Omega = \langle \omega\phi, \nabla \cdot \nabla_\perp \omega \rangle_\Omega - \langle \phi \times \nabla_\perp \omega, \nabla_\perp \omega \rangle_\Omega \tag{3.25}$$

Where integration by parts and the homogeneous boundary conditions were used. This is equal to zero, since $\nabla \cdot \nabla_\perp(\cdot) = 0$ and $\phi \times \nabla_\perp \omega \perp \nabla_\perp \omega$. Using integration by parts on the third term of equation (3.23) yields,

$$\langle \nabla \times \nabla_\perp \omega, \omega \rangle_\Omega = \langle \nabla_\perp \omega, \nabla_\perp \omega \rangle_\Omega - \int_{\partial\Omega} \omega(\nabla_\perp \omega \times \vec{n}) \tag{3.26}$$

The first term is twice the total palinstrophy, $P = \frac{1}{2}\langle \nabla_\perp \omega^h, \nabla_\perp \omega^h \rangle_\Omega$ and the boundary term is zero for homogeneous boundary conditions. Thus withou8t an external force this yields the conservation equation,

$$\frac{\partial E}{\partial t} = -2\mathrm{Re}^{-1} P \tag{3.27}$$

Where we have used the relation $\nabla \times \nabla(\cdot) = 0$ for the pressure term.

3.3. weak form

We can write equations (3.1-3.5) into the weak form,

$$\text{Find } \vec{u} \in H(\mathrm{div}, \Omega) \cap H(\mathrm{rot}, \Omega),\ \omega \in H(\mathrm{curl}, \Omega) = H^1(\Omega) \text{ and } P \in H^1(\Omega) \tag{3.28}$$

$$\begin{cases} \langle \frac{\partial \vec{u}}{\partial t}, \vec{v} \rangle_\Omega + \langle \omega \times \vec{u}, \vec{v} \rangle_\Omega + \mathrm{Re}^{-1} \langle \nabla_\perp \omega, \vec{v} \rangle_\Omega + \langle \nabla P, \vec{v} \rangle_\Omega = \langle \vec{f}, \vec{v} \rangle_\Omega, \forall \vec{v} \in [L^2(\Omega)]^2 \\ \langle \omega, w \rangle_\Omega - \langle \nabla \times \vec{u}, w \rangle_\Omega = 0, \forall w \in L^2(\Omega) \\ \langle \nabla \cdot \vec{u}, q \rangle_\Omega = 0, \forall q \in L^2(\Omega). \\ \vec{u} \cdot \hat{n} = \vec{u}_\parallel, \text{ on } \Gamma \times (0, T] \\ \vec{u} \times \hat{n} = \vec{u}_\perp, \text{ on } \Gamma \times (0, T]. \end{cases} \tag{3.29}$$

Where the spaces where chosen to guarantee the convergence of the integrals. But $\vec{u} \in H(\text{div},\Omega) \cap H(\text{rot},\Omega)$, $\omega \in H(\text{curl},\Omega) = H^1(\Omega)$ and $P \in H^1(\Omega)$ is too restrictive for the basis functions as explained in section 2.4.1. Therefor we will change some differential operators to their weak counterparts.

We will decide our solution and test spaces based on the Hilbert complexes discussed in section 2.3. Since u is a vector it needs to be either in $H(\text{rot},\Omega)$ or $H(\text{div},\Omega)$. To ensure mass conservation we need $\langle \nabla \cdot \vec{u}, q \rangle_\Omega = 0$ to be exactly satisfied and therefor we need $u \in H(\text{div},\Omega)$. This will be expaneded on in the next section. Now in order to apply the finite element method as described in section 2.4 we need $\vec{v}$ in the same space as $\vec{u}$, w in the same space as ω and q in the same space as P. Further more we need to compute $\langle \nabla \times \vec{u}, w \rangle_\Omega$, but $u \in H(\text{div},\Omega)$, so this can only be done weakly. But then $\langle \tilde{\nabla} \times \vec{u}, w \rangle_\Omega$ implies that $w \in H(\text{curl},\Omega)$. And therefor als $\omega \in H(\text{curl},\Omega)$. Similarly the term $\langle \nabla P, \vec{v} \rangle_\Omega$ means that ∇P needs to be in the same space as $\vec{v}$, $H(\text{div},\Omega)$. From the Hilbert complexes it follows that this is only possible if we change the ∇ to a $\tilde{\nabla}$ and pick $P \in L^2(\Omega)$. Lastly $\langle \nabla \cdot \vec{u}, q \rangle_\Omega$ means that we need $q \in L^2(\Omega)$.

Applying these spaces and working out the weak operators results in:

$$\text{Find } (\vec{u}, \omega, P) \in H(\text{div},\Omega) \times H^1(\Omega) \times L^2(\Omega) \text{ such that}$$
$$\begin{cases} \langle \dfrac{\partial \vec{u}}{\partial t}, \vec{v} \rangle_\Omega + \langle \omega \times \vec{u}, \vec{v} \rangle_\Omega + \text{Re}^{-1} \langle \nabla_\perp \omega, \vec{v} \rangle_\Omega - \langle P, \nabla \cdot \vec{v} \rangle_\Omega = \langle \vec{f}, \vec{v} \rangle_\Omega, \forall \vec{v} \in \text{H(div},\Omega) \\ \langle \omega, w \rangle_\Omega - \langle \vec{u}, \nabla_\perp w \rangle_\Omega = -\displaystyle\int_\Gamma w u_\parallel \, d\Gamma, \forall w \in \text{H(curl},\Omega) \\ \langle \nabla \cdot \vec{u}, q \rangle_\Omega = 0, \forall q \in \text{L}^2(\Omega). \end{cases} \tag{3.30}$$

3.4. Spatial discretization

As discussed in section 2.4.1, we now pick Continuous Lagrange elements of degree N for ω and w, the Raviart-Thomas elements of degree N for $\vec{u}$ and $\vec{v}$, and the discontinuous Lagrange elements for p and q. The only essential boundary conditions we have here are $\vec{u} \cdot \vec{n}$ on $\partial\Omega$. Therefor we replace H(div,Ω) by $V_E^h = \{\vec{v} \in V^h : \vec{v} \cdot \vec{n} = u_\perp\}$, H(curl,$\Omega$) by W^h and $L^2(\Omega)$ by Q^h.

$$\text{Find } (\vec{u}^h, \omega, P) \in V_E^h \times W^h \times Q^h \text{ such that}$$
$$\langle \frac{\partial \vec{u}^h}{\partial t}, \vec{v}^h \rangle_\Omega + \langle \omega^h \times \vec{u}^h, \vec{v}^h \rangle_\Omega + \text{Re}^{-1} \langle \nabla_\perp \omega^h, \vec{v}^h \rangle_\Omega - \langle P^h, \nabla \cdot \vec{v}^h \rangle_\Omega = \langle \vec{f}, \vec{v}^h \rangle_\Omega, \forall \vec{v}^h \in V_0^h \tag{3.31}$$
$$\langle \omega^h, \xi^h \rangle_\Omega - \langle \vec{u}^h, \nabla_\perp \xi^h \rangle_\Omega = -\int_\Gamma \xi^h u_\parallel \, d\Gamma, \forall \xi^h \in W^h \tag{3.32}$$
$$\langle \nabla \cdot \vec{u}^h, q^h \rangle_\Omega = 0, \forall q^h \in Q^h. \tag{3.33}$$

Where $V_0^h = \{\vec{v} \in V^h : \vec{v} \cdot \vec{n} = 0\}$ Or in the form of the basis functions,

$$\begin{cases} \displaystyle\sum_{i=1}^{n_u} \frac{\partial u_i}{\partial t} \langle \vec{v}_i, \vec{v}_j \rangle_\Omega + \sum_{i,k=1}^{n_u,n_\omega} u_i \omega_k \langle \xi_k \times \vec{v}_i, \vec{v}_j \rangle + \frac{1}{Re} \sum_{i=1}^{n_\omega} \omega_i \langle \nabla_\perp \xi_i, \vec{v}_j \rangle - \sum_{i=1}^{n_p} p_i \langle q_i, \nabla \cdot \vec{v}_j \rangle = \langle \vec{f}, \vec{v}_j \rangle_\Omega, \qquad j = 1, \ldots, n_{u,E}. \\ \displaystyle\sum_{i=1}^{n_u} u_i \langle \vec{v}_i, \nabla \times \vec{\xi}_j \rangle - \sum_{i=1}^{n_\omega} \omega_i \langle \xi_i, \xi_j \rangle + \int_{\partial\Omega} \xi_j (u_\parallel \times \hat{n}) \, d\Gamma = 0, , \qquad j = 1, \ldots, n_\omega. \\ \displaystyle\sum_{i=1}^{n_u} u_i \langle \nabla \cdot \vec{v}_i, q_j \rangle = 0, , \qquad j = 1, \ldots, n_P. \end{cases} \tag{3.34}$$

Where $\vec{v}_i$ are the Raviart-Thomas basis functions, ξ_i are the continuous Lagrange basis functions and q_i are the discontinuous Lagrange basis functions. And n_u, n_ω and n_P are the degrees of freedom for $\vec{u}$, ω and P respectivally and $n_{u,E}$ are the degrees of freedom of u after removing the degrees of freedom used for the essential boundary condition.

3.5. Semi-Discrete Conservation properties

In this section we will discuss the conservational properties of the discrete Navier-Stokes equation as described in equations (3.31-3.33). We will prove them only for the case homogeneous boundary conditions, thus $V_E^h = V^h$ and $V_0^h = V^h$. For a further discussion see [14].

3.5.1. Mass conservation

Mass conservation for the continuous case follows from the divergence free property of $\vec{u}$. For our discrete approximation $\vec{u}^h$ the divergence free property is strongly satisfied. Therefor mass is also conserved discretely.

3.5.2. Energy conservation

Equation (3.31) is valid for all $\vec{v}^h \in V^h$, therefore it is also valid for $\vec{u}^h \in V^h$ (these spaces are the same, since the boundary values are homogeneous),

$$\langle \frac{\partial \vec{u}^h}{\partial t}, \vec{u}^h \rangle_\Omega + \langle \omega^h \times \vec{u}^h, \vec{u}^h \rangle_\Omega + \mathrm{Re}^{-1} \langle \nabla_\perp \omega^h, \vec{u}^h \rangle_\Omega - \langle P^h, \nabla \cdot \vec{u}^h \rangle_\Omega + \int_{\partial\Omega} P u_\parallel d\Gamma = \langle \vec{f}, \vec{u}^h \rangle_\Omega \tag{3.35}$$

We will analyse this term by term. The first term is simply the change in discrete kinetic energy, $\frac{\partial K^h}{\partial t}$. The second term is zero since $\omega^h \times \vec{u}^h \perp \vec{u}^h$. Using integration by parts on the second term yields,

$$\langle \nabla_\perp \omega^h, \vec{u}^h \rangle_\Omega = \langle \omega^h, \nabla \times \vec{u}^h \rangle_\Omega \tag{3.36}$$

Where $\langle \omega^h, \nabla \times \vec{u}^h \rangle_\Omega = \langle \omega^h, \omega^h \rangle_\Omega = 2E^h$ and $\int_{\partial\Omega} \omega u_\perp d\Omega = 0$ if $u_\perp = 0$. The third term of equation (3.35) is equal to zero, since the divergence free property of u^h is strongly enforced. And the last term is zero will be zero if there is no external force.

3.5.3. Vorticity

Equation (3.31) holds for all $\vec{v}^h \in V^h$ and if $\xi^h \in W^h$, then $\nabla_\perp \xi^h \in V^h$, thus equation (3.31) holds for $\nabla_\perp \xi$.

$$\langle \frac{\partial \vec{u}^h}{\partial t}, \nabla_\perp \xi^h \rangle_\Omega + \langle \omega^h \times \vec{u}^h, \nabla_\perp \xi^h \rangle_\Omega + \mathrm{Re}^{-1} \langle \nabla_\perp \omega^h, \nabla_\perp \xi^h \rangle_\Omega - \langle P^h, \nabla \cdot \nabla_\perp \xi^h \rangle_\Omega = \langle \vec{f}, \nabla_\perp \xi^h \rangle_\Omega, \forall \xi^h \in W^h \tag{3.37}$$

Applying integration by parts on the first term yields,

$$\langle \frac{\partial \vec{u}^h}{\partial t}, \nabla_\perp \xi^h \rangle_\Omega = \langle \nabla \times \frac{\partial \vec{u}^h}{\partial t}, \xi^h \rangle_\Omega + \int_{\partial\Omega} \xi^h u_\parallel d\Gamma \tag{3.38}$$

Plugging the equation above into each other and substituting $\xi^h = 1 \in W^h$ yields,

$$\langle \nabla \times \frac{\partial \vec{u}^h}{\partial t}, 1 \rangle_\Omega + \int_{\partial\Omega} u_\parallel d\Gamma = 0 \tag{3.39}$$

But the first term here is the change in vorticity, and the other term is 0, if $u_\parallel = 0$, thus vorticity is conserved.

3.5.4. Enstrophy

Taking the time derivative of (3.32) yields,

$$\langle \frac{\partial \omega^h}{\partial t}, \xi^h \rangle_\Omega - \langle \frac{\partial \vec{u}^h}{\partial t}, \nabla_\perp \xi^h \rangle_\Omega = -\int_\Gamma \xi^h \frac{\partial u_\parallel}{\partial t} d\Gamma = 0, \forall \xi^h \in W^h \tag{3.40}$$

Where $u_\parallel = 0$ for homogeneous boundary conditions was used. Plugging this into equation (3.37) yields,

$$\langle \frac{\partial \omega^h}{\partial t}, \xi^h \rangle_\Omega + \langle \omega^h \times \vec{u}^h, \nabla_\perp \xi^h \rangle_\Omega + \mathrm{Re}^{-1} \langle \nabla_\perp \omega^h, \nabla_\perp \xi^h \rangle_\Omega - \langle P^h, \nabla \cdot \nabla_\perp \xi^h \rangle_\Omega = \langle \vec{f}, \nabla_\perp \xi^h \rangle_\Omega, \forall \xi^h \in W^h \tag{3.41}$$

Here the fourth term is zero since, $\nabla \cdot \nabla_\perp(\cdot) = 0$. Since $\omega^h \in W^h$, the equation above also holds for ω^h,

$$\langle \frac{\partial \omega^h}{\partial t}, \omega^h \rangle_\Omega + \langle \omega^h \times \vec{u}^h, \nabla_\perp \omega^h \rangle_\Omega + \mathrm{Re}^{-1} \langle \nabla_\perp \omega^h, \nabla_\perp \omega^h \rangle_\Omega = \langle \vec{f}, \nabla_\perp \omega^h \rangle_\Omega \tag{3.42}$$

We will again analyse this equation term by term. The first term is the change in total enstrophy $\frac{\partial E}{\partial t}$. Since $\vec{u} \in V^h$ and $\nabla \cdot \vec{u} = 0$ is satisfied strong, we are able to write $\vec{u}^h = \nabla_\perp \phi^h$, were $\phi \in W^h$. Times means that we can rewrite the second equation as,

$$\langle \omega^h \times \vec{u}^h, \nabla_\perp \omega^h \rangle_\Omega = \langle \nabla \cdot (\omega^h \phi^h), \nabla_\perp \omega \rangle_\Omega - \langle \phi^h \times \nabla_\perp \omega^h, \nabla_\perp \omega^h \rangle_\Omega = \langle \omega^h \phi^h, \nabla \cdot \nabla_\perp \omega \rangle_\Omega - \langle \phi \times \nabla_\perp \omega, \nabla_\perp \omega^h \rangle_\Omega \quad (3.43)$$

Where integration by parts and the homogeneous boundary conditions were used. This is equal to zero, since $\nabla \cdot \nabla_\perp(\cdot) = 0$ and $\phi^h \times \nabla_\perp \omega^h \perp \nabla_\perp \omega^h$. The third term is twice the total palinstrophy, $P = \frac{1}{2}\langle \nabla_\perp \omega^h, \nabla_\perp \omega^h \rangle_\Omega$. This leaves us with the conservation equation. And the forth term is, ofcourse, zero when there is no external force. This leaves us with the conservation equation.

$$\frac{\partial E}{\partial t} = -2\mathrm{Re}^{-1} P. \quad (3.44)$$

This means that when there is no external body force, Enstrophy is conserved in the inviscid limit (when $Re \to \infty$).

3.6. Time discretization

Applying the midpoint method and midpoint rule to (3.34), results in:

$$\begin{cases} \sum_{i=1}^{n_u} \frac{u_i^{t+1} - u_i^t}{\Delta t} \langle \vec{v}_i, \vec{v}_j \rangle_\Omega + \sum_{i,k=1}^{n_u, n_\omega} \frac{u_i^{t+1} + u_i^t}{2} \frac{\omega_k^{t+1} + \omega_k^t}{2} \langle \xi_k \times \vec{v}_i, \vec{v}_j \rangle + \frac{1}{Re} \sum_{i=1}^{n_\omega} \frac{\omega_i^{t+1} + \omega_i^t}{2} \langle \nabla \times \xi_i, \vec{v}_j \rangle - \sum_{i=1}^{n_p} \frac{p_i^{t+1} + p_i^t}{2} \langle q_i, \nabla \cdot \vec{v}_j \rangle \\ = \langle \vec{f}, \vec{v}_j \rangle_\Omega, \qquad j = 1, \ldots, n_{u,E}. \\ \sum_{i=1}^{n_u} u_i^{t+1} \langle \vec{v}_i, \nabla \times \vec{\xi}_j \rangle - \sum_{i=1}^{n_\omega} \omega_i^{t+1} \langle \xi_i, \xi_j \rangle - \int_\Gamma \xi_j (u_\parallel \times \hat{n}) d\Gamma = 0, , \qquad j = 1, \ldots, n_\omega. \\ \sum_{i=1}^{n_u} u_i^{t+1} \langle \nabla \cdot \vec{v}_i, q_j \rangle = 0, , \qquad j = 1, \ldots, n_P. \end{cases} \quad (3.45)$$

Where u_i^t is the coëfficient for the basis function $\vec{v}_i$ in the finite element approximation for $\vec{u}$ at timestep t. And similarly p_i^t, ω_i^t are the coefficients for the basis functions q_i, ξ_i, respectivally, at time step t.

We can rewrite equation (3.45) as:

$$\begin{cases} F_j^u(\boldsymbol{u}^{t+1}, \boldsymbol{\omega}^{t+1}, \boldsymbol{P}^{t+1}, \boldsymbol{u}^t, \boldsymbol{\omega}^t, \boldsymbol{P}^t) = \sum_{i=1}^{n_u} \frac{u_i^{t+1} - u_i^t}{\Delta t} \langle \vec{v}_i, \vec{v}_j \rangle_\Omega + \sum_{i,k=1}^{n_u, n_\omega} \frac{u_i^{t+1} + u_i^t}{2} \frac{\omega_k^{t+1} + \omega_k^t}{2} \langle \xi_k \times \vec{v}_i, \vec{v}_j \rangle + \frac{1}{Re} \sum_{i=1}^{n_\omega} \frac{\omega_i^{t+1} + \omega_i^t}{2} \langle \nabla \times \xi_i, \vec{v}_j \rangle \\ - \sum_{i=1}^{n_p} \frac{p_i^{t+1} + p_i^t}{2} \langle q_i, \nabla \cdot \vec{v}_j \rangle - \langle \vec{f}, \vec{v}_j \rangle_\Omega = 0, \qquad j = 1, \ldots, n_{u,E}. \\ F_j^\omega(\boldsymbol{u}^{t+1}, \boldsymbol{\omega}^{t+1}, \boldsymbol{P}^{t+1}, \boldsymbol{u}^t, \boldsymbol{\omega}^t, \boldsymbol{P}^t) = \sum_{i=1}^{n_u} u_i^{t+1} \langle \vec{v}_i, \nabla \times \vec{\xi}_j \rangle - \sum_{i=1}^{n_\omega} \omega_i^{t+1} \langle \xi_i, \xi_j \rangle - \int_\Gamma \xi_j (u_\parallel \times \hat{n}) d\Gamma = 0, , \qquad j = 1, \ldots, n_\omega. \\ F_j^P(\boldsymbol{u}^{t+1}, \boldsymbol{\omega}^{t+1}, \boldsymbol{P}^{t+1}, \boldsymbol{u}^t, \boldsymbol{\omega}^t, \boldsymbol{P}^t) = \sum_{i=1}^{n_u} u_i^{t+1} \langle \nabla \cdot \vec{v}_i, q_j \rangle = 0, , \qquad j = 1, \ldots, n_P. \end{cases} \quad (3.46)$$

Where

$$\boldsymbol{u}^t = \begin{bmatrix} u_1^t \\ u_2^t \\ \cdots \\ u_{n_u}^t \end{bmatrix}, \boldsymbol{\omega}^t = \begin{bmatrix} \omega_1^t \\ \omega_2^t \\ \cdots \\ \omega_{n_\omega}^t \end{bmatrix}, \boldsymbol{P}^t = \begin{bmatrix} p_1^t \\ p_2^t \\ \cdots \\ p_{n_u}^t \end{bmatrix}. \quad (3.47)$$

Unlike for the primal and mixed heat equation this doesn't result in a bilinear system of equations. We are left with the non linear term $\langle \omega \times \vec{u}, \vec{v} \rangle$. Therefor we are unable to immediately calculate $(\vec{u}^{t+1}, \omega^{t+1}, p^{t+1})$ from $(\vec{u}^t, \omega^t, p^t)$. We will therefor use the Newton-Raphson method. The Newton-Raphson method allows us to approximate roots of functions through iteration, as long as our initial guess is sufficiently close to the root. In this way, if we know $(\boldsymbol{u}^t, \boldsymbol{\omega}^t, \boldsymbol{P}^t)$, we can find the roots of equation (3.46), and thereby find $(\boldsymbol{u}^{t+1}, \boldsymbol{\omega}^{t+1}, \boldsymbol{P}^{t+1})$.

The Newton-Raphson method now states that each next iteration is given by the previous iteration in the following manner:

$$\begin{bmatrix} \boldsymbol{u}_{n+1}^{t+1} \\ \boldsymbol{\omega}_{n+1}^{t+1} \\ \boldsymbol{P}_{n+1}^{t+1} \end{bmatrix} = \begin{bmatrix} \boldsymbol{u}_{n}^{t+1} \\ \boldsymbol{\omega}_{n}^{t+1} \\ \boldsymbol{P}_{n}^{t+1} \end{bmatrix} - \mathbf{J}^{-1}(\boldsymbol{u}_n^{t+1}, \boldsymbol{\omega}_n^{t+1}, \boldsymbol{P}_n^{t+1}, \boldsymbol{u}^t, \boldsymbol{\omega}^t, \boldsymbol{P}^t) \begin{bmatrix} \boldsymbol{F}^u(\boldsymbol{u}_n^{t+1}, \boldsymbol{\omega}_n^{t+1}, \boldsymbol{P}_n^{t+1}, \boldsymbol{u}^t, \boldsymbol{\omega}^t, \boldsymbol{P}^t) \\ \boldsymbol{F}^\omega(\boldsymbol{u}_n^{t+1}, \boldsymbol{\omega}_n^{t+1}, \boldsymbol{P}_n^{t+1}, \boldsymbol{u}^t, \boldsymbol{\omega}^t, \boldsymbol{P}^t) \\ \boldsymbol{F}^P(\boldsymbol{u}_n^{t+1}, \boldsymbol{\omega}_n^{t+1}, \boldsymbol{P}_n^{t+1}, \boldsymbol{u}^t, \boldsymbol{\omega}^t, \boldsymbol{P}^t) \end{bmatrix} \tag{3.48}$$

Where $(\boldsymbol{u}^{t+1}, \boldsymbol{\omega}_n^{t+1}, \boldsymbol{P}_n^{t+1})$ is the previous iteration, $\mathbf{J}^{-1}$ is the inverse of the Jacobian, which be written in the form of 9 sub matrices in the following manner:

$$\mathbf{J}(\boldsymbol{u}_n^{t+1}, \boldsymbol{\omega}_n^{t+1}, \boldsymbol{P}_n^{t+1}, \boldsymbol{u}^t, \boldsymbol{\omega}^t, \boldsymbol{P}^t) = \begin{bmatrix} \frac{\partial \boldsymbol{F}^u}{\partial \boldsymbol{u}} & \frac{\partial \boldsymbol{F}^u}{\partial \boldsymbol{\omega}} & \frac{\partial \boldsymbol{F}^u}{\partial \boldsymbol{P}} \\ \frac{\partial \boldsymbol{F}^\omega}{\partial \boldsymbol{u}} & \frac{\partial \boldsymbol{F}^\omega}{\partial \boldsymbol{\omega}} & \frac{\partial \boldsymbol{F}^\omega}{\partial \boldsymbol{P}} \\ \frac{\partial \boldsymbol{F}^P}{\partial \boldsymbol{u}} & \frac{\partial \boldsymbol{F}^P}{\partial \boldsymbol{\omega}} & \frac{\partial \boldsymbol{F}^P}{\partial \boldsymbol{P}} \end{bmatrix} \tag{3.49}$$

Where $\frac{\partial \boldsymbol{F}^u}{\partial \boldsymbol{u}}$ is a $n_u \times n_u$ sub matrix with $(\frac{\partial \boldsymbol{F}^u}{\partial \boldsymbol{u}})_{ij} = \frac{\partial F_i^u}{\partial u_j}$, $\frac{\partial \boldsymbol{F}^u}{\partial \boldsymbol{\omega}}$ is a $n_\omega \times n_u$ sub matrix with $(\frac{\partial \boldsymbol{F}^u}{\partial \boldsymbol{\omega}})_{ij} = \frac{\partial \boldsymbol{F}_i^u}{\partial \omega_j}$ $\frac{\partial \boldsymbol{F}^u}{\partial \boldsymbol{P}}$ is a $n_p \times n_u$ sub matrix with $(\frac{\partial \boldsymbol{F}^u}{\partial \boldsymbol{P}})_{ij} = \frac{\partial \boldsymbol{F}_i^u}{\partial p_j}$, $\frac{\partial \boldsymbol{F}^\omega}{\partial \boldsymbol{u}}$ is a $n_u \times n_\omega$ matrix with $(\frac{\partial \boldsymbol{F}^\omega}{\partial \boldsymbol{u}})_{ij} = \frac{\partial \boldsymbol{F}_i^\omega}{\partial u_j}$ etc.

If we take the values of the previous time step, $(\boldsymbol{u}^t, \boldsymbol{\omega}^t, \boldsymbol{P}^t)$, as our initial guess for the values of the next timestep, $\boldsymbol{u}_0^{t+1}, \boldsymbol{\omega}_0^{t+1}, \boldsymbol{P}_0^{t+1})$, we can use the Newton-Raphson method to iterate to the correct values of the next time step, since this should be a good enough inital guess for a suffiecntly small timestep.

4

Results and discussion

4.1. Steady Heat equations

We looked at the convergence of the primal and mixed steady heat equation as described in sections 2.4.2 and 2.4.3. We did this by looking at the problem

$$\begin{cases} -\nabla \cdot \nabla u = -\sin(x) - \cos(y) \text{ on } (0,\pi) \times (0,\pi) \\ \nabla u \cdot \vec{n} = 1 \text{ on } \{0\} \times [0,\pi] \cup \{1\} \times [0,\pi] \\ u = -\sin(x) - \cos(y) \text{ on } (0,\pi) \times \{0\} \cup (0,\pi) \times \{1\} \end{cases} \tag{4.1}$$

Where we know that the exact solution is $u_{\text{exact}} = -\sin(x) - \cos(y)$. This problem was chosen so that the exact solution is known, and to test if the convergence rate is as expected. This is done to see if the method is working as expected. We approximated the solution to this problem with the Julia programming language[3], using the Gridap module[2][18]. We used a square mesh from sizes 4 by 4, 8 by 8, 16, by 16, 32 by 32 and 64 by 64. And used this mesh with the primal steady heat equation with Continuous Lagrange elements of 1 and 2 and for the mixed formulation with discontinuous Lagrange elements of order 1 together with Raviart-Thomas elements of order 2 and with discontinuous Lagrange elements of order 2 with Raviart-Thomas elements of order 3. We then calculated the total root mean square error for these different mesh sizes. The results can be seen in figure 4.1, where the lines the lines $y = (1/N)^2$ and $y = (1/N)^3$ are added to show the degree of convergence. This is to be expected, since we expect the error to converge at a rate proportional to the the step size to the power of the order + 1, error $\propto (1/N)^{(\text{order}+1)}$ [1, p. 59]

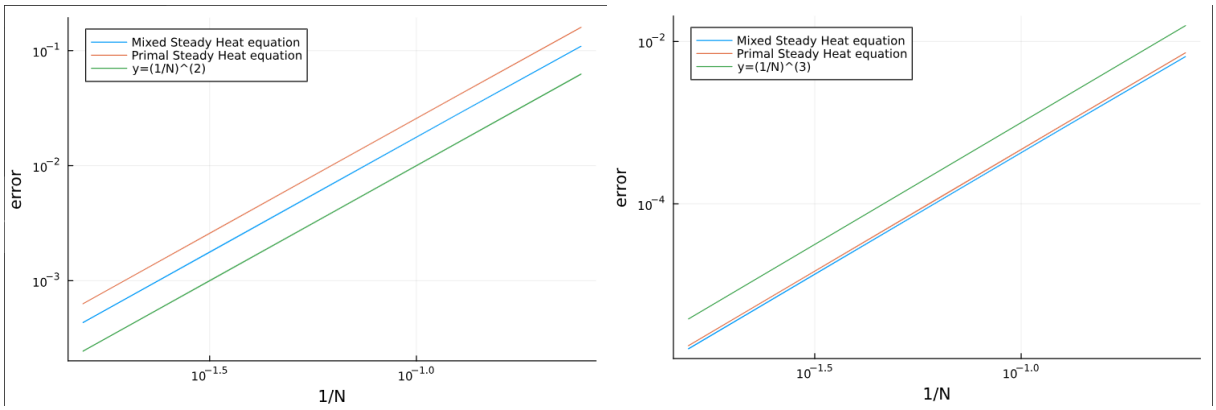

(a) Order 1 Continuous Lagrange elements were used for the Primal formulation and order 1 Discontinuous lagrange elements together with order 2 Raviart-Thomas elements for the Mixed formulation

(b) Order 2 Continuous Lagrange elements were used for the Primal formulation and order 2 Discontinuous lagrange elements together with order 3 Raviart-Thomas elements for the Mixed formulation

Figure 4.1: Root mean square error of the finite element approximation for different mesh sizes

4.2. Unsteady heat equation

The transient heat equation was also implemented in Gridap, but due to time restrictions the results are ommitted.

4.3. Navier-Stokes equations

The conservative discretization, as described in the previous chapter, was tested for the lid driven cavity problem. This problem is describes a square box, with non-slip boundaries, where all boundaries are not moving, except for the top, which moves with a constant velocity of 1 to the left. This can be described as follows,

$$\frac{\partial \vec{u}}{\partial t} + \omega \times \vec{u} + \mathrm{Re}^{-1}\nabla_{\perp}\omega + \nabla P = 0, \text{ in } (0,1)\times(0,1)\times(0,T] \tag{4.2}$$

$$\omega - \nabla \times \vec{u} = 0, \text{ in } (0,1)\times(0,1)\times(0,T] \tag{4.3}$$

$$\nabla \cdot \vec{u} = 0, \text{ in } (0,1)\times(0,1)\times(0,T] \tag{4.4}$$

$$\vec{u}\cdot\hat{n} = 0, \text{ on } \{0,1\}\times[0,1]\cup[0,1]\times\{0,1\}\times(0,T] \tag{4.5}$$

$$\vec{u}\times\hat{n} = -1, \text{ on } [0,1]\times\{1\}\times(0,T]. \tag{4.6}$$

$$\vec{u}\times\hat{n} = 0, \text{ on } \{0,1\}\times[0,1]\cup[0,1]\times\{0\}\times(0,T]. \tag{4.7}$$

Where, without loss of generality we have taken the length of the box to be 1. Where for a small enough Reynolds number this should lead to a steady state after sufficient time. Thus by repeating the time iteration, as described in the previous chapter, until the difference between two subsequent time steps is sufficiently small gives us an approximation for that steady state. We first implemented this process in the Julia programming language[3], using the Gridap[2][18] module, but this implementation was too slow to work with. We then implemented this process in Python, using the firedrake system[8]. The results will be compared to some benchmark cases[15][4].

We pciked a 38 by 38 mesh, with elements of order 3 (meaning order 3 continuous lagrange elements, order 3 Raviart-Thomas elements and order 2 discontinuous lagrange elements), Reynolds number 1000, a difference of 10^{-12} for subsequent Newton-Raphson steps before moving to the next time step, and step size $\Delta t = 0.01$. The resulting steady state is compared to a benchmark case. The benchmark solutions were produced, three different large (graded) grids were used (of sizes 1201x1201, 1413x1413 and 1661x1661) and the extrapolated result was projected (interpolated) onto the base 1201x1201 grid[15].

In figure 4.2 we show contours representing vorticity values of -5 to 5 with steps of 1 for the conservative discretization and the benchmark. We see that the contours match very well. Only in the top right the structure preserving model has some results that don't match well. Furthermore, in figure 4.3 the x-component of the velocity along the vertical line x=0.5 for this case is compared to the benchmark. And it is again shown that it matches up very well.

4.3.1. Altered mesh

To try to improve the accuracy we used a different type of mesh, with higher resolution near the boundary and lower resolution in the centre, since the biggest changes happen near the boundary. This new mesh is made in the following manner. First an N by N triangular mesh, made up of squares separated by a line from the top left to bottom right AND a line from the top right to bottom left. Then the new mesh is made with the following mapping,

$$\begin{aligned} m : (\bar{x},\bar{y}) &\to (x,y) \text{ such that} \\ x &= 0.5(\sin((\bar{x}-\frac{1}{2})\pi)+1) \\ y &= 0.5(\sin((\bar{y}-\frac{1}{2})\pi)+1) \end{aligned}$$

Here x, y are the coördinates of the altered mesh and $\bar{x},\bar{y}$ are the coördinates of the old mesh. A 36 by 36 example can be seen in figure 4.4.

We test the accuracy of this 36 by 36 altered mesh with Reynolds number 2500 against a benchmark generateed in the sameway as before [15]. Again elements of order 3, Newton-Raphson tollerance 10^{-12} and time

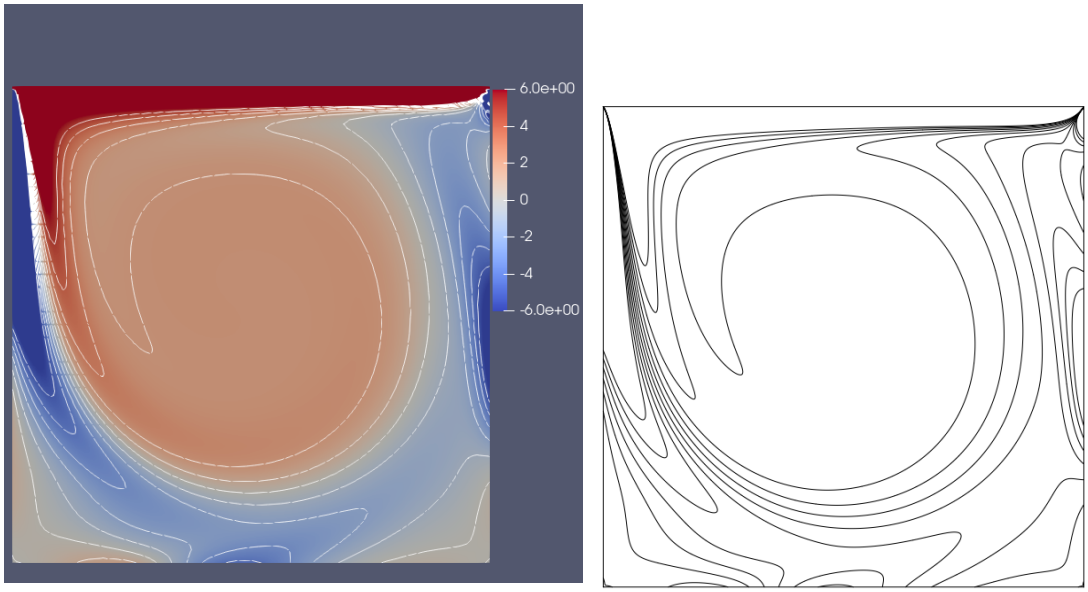

(a) Countours representing vorticity values from -5 to 5 at steps of 1 for the structure preserving grid with a 38 by 38 mesh, with elements of order 3 and Re=1000

(b) Countours representing vorticity values from -5 to 5 at steps of 1 given by the benchmark[15] for Re=1000

Figure 4.2: Comparison between the conservative discretization and a benchmark case of vorticity countours

steps of 0.01 were used. Figure 4.5 shows contours representing vorticity values of -5 to 5 with steps of 1 for the method and a benchmark. Here there is a noticeable difference in the centre between the contour lines, but they match quite well near the edge, even at the top right corner. This is expected since the mesh has a higher resolution near the boundary.
Figure 4.6 shows the x-component of the velocity along the line x=0.5 of this method compared to a benchmark for Reynolds number 2500. We see that this method preforms well very close to the boundary, but over or under estimates just a bit further from the boundary. This is could be explained by the chosen mesh having a higher resolution close to the boundary. It also matches the benchmark near the centre, this could be the case because there is little movement in the centre.

4.3.2. Comparison to Taylor-Hood

We now compare our conservative discretization to Taylor-Hood method. In order to do so we pick the same mesh, a triangular mesh made up of 28 by 28 squares, separated into triangles by a line from the top left to the bottom right. The conservative discretization will have elements of order 2 (meaning order 2 continuous lagrange elements, order 2 Raviart-Thomas elements and order 1 discontinuous lagrange elements). Similarly, the Taylor-Hood method will have order 2 for velocity in all direction and order 1 for pressure. And we take the same time step $\Delta t = 0.01s$. The results for $t = 1$, $t = 3$ and $t = 5$ can be seen in figure 4.7. We see that in the the Taylor-Hood method has some oscillations in the top left, which are not based on anything physical, while the structure conserving method does not have these errors. This shows a clear advantage of the conservative discretization.

For an additional comparison, in figure 4.8 we shown the results of the conservative discretization on an altered mesh with a 28 by 28 mesh with polynomial order 2 and the same step size next to a reference method, which is a conservative discretization with normal mesh of size 50 by 50 and order 3. This reference method is the conservative discretization on a normal 50 by 50 grid, with order 3. This increased order, means that it's the closest to the actual result. We see smoother results for the altered mesh near the boundary, especially near the top right corner, which matches the higher resolution reference better than any other method. There is no noticeable difference in the rest of the figure.

Lastly we compare some initial time step for the lid driven cavity problem for Reynolds number 10000 in figure 4.9. We compare the conservative discretization and the Taylor-Hood method both on 50 by 50 version of the original mesh. Both with polynomial order 3 and time step 0.01. As a reference we also show the results of a higher resolution Taylor-Hood method. This reference has order 3 and a 200 by 200 mesh.
Here we see that the conservative discretization matches the reference for longer. It also at no point gets the

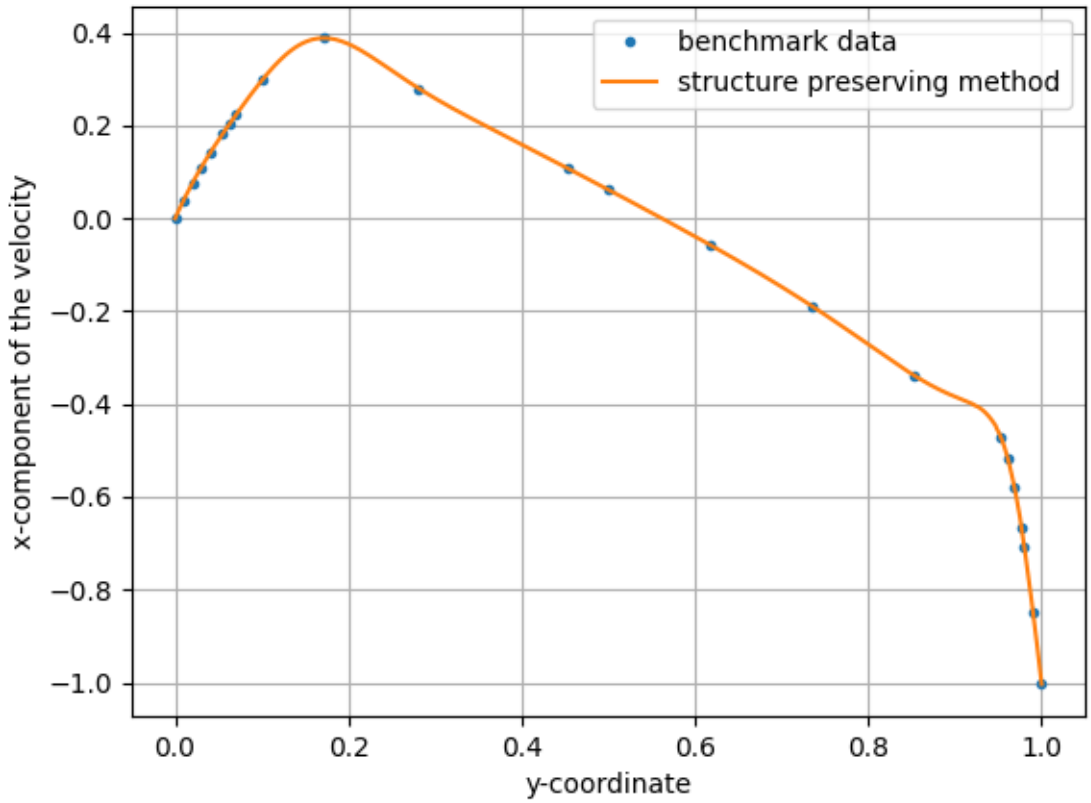

[width=8cm]

Figure 4.3: Comparison of the x-component of the velocity along the line x=0.5 for Re=1000

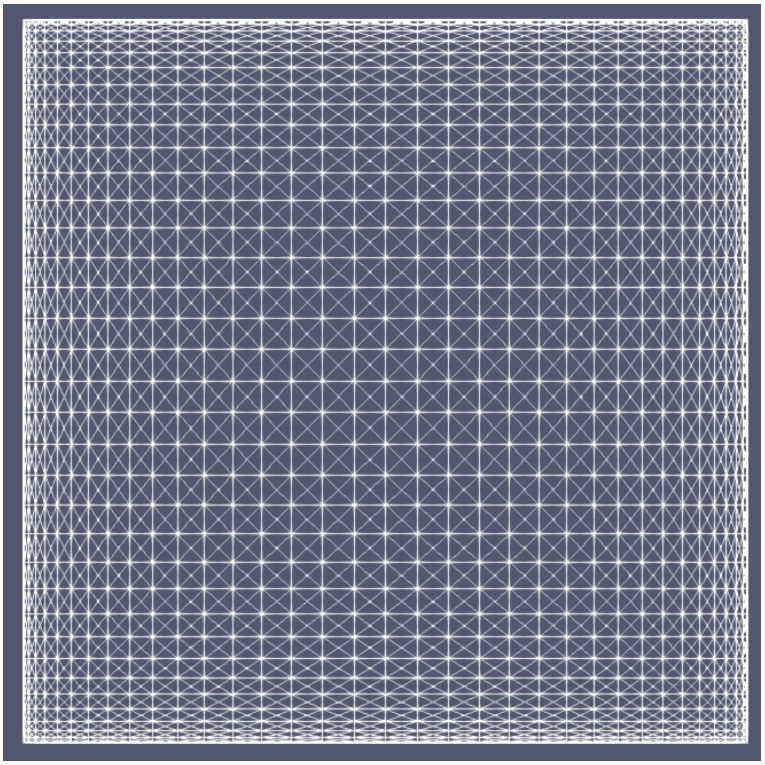

Figure 4.4: A 36 by 36 example of the altered mesh.

unphysical oscilations in the velocity as the Taylor-Hood method does. This shows an even clearer advantage of the conservative discretization.

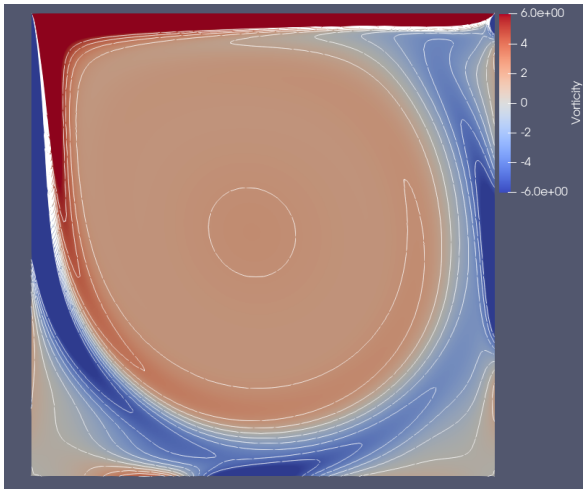

(a) Countours representing vorticity values from -5 to 5 at steps of 1 for the structure preserving grid with a 36 by 36 mesh, with elements of order 3 and Re=2500

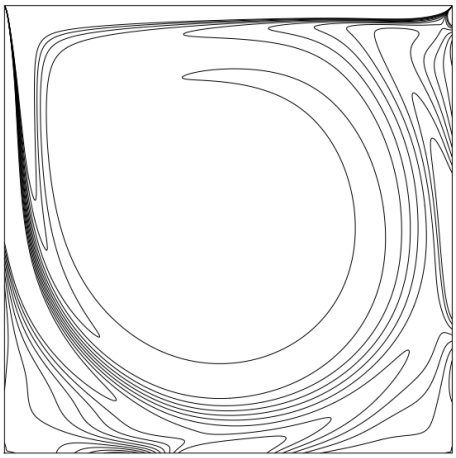

(b) Countours representing vorticity values from -5 to 5 at steps of 1 given by the benchmark[15] for Re=2500

Figure 4.5: Comparison between the conservative discretization and a benchmark case of vorticity countours

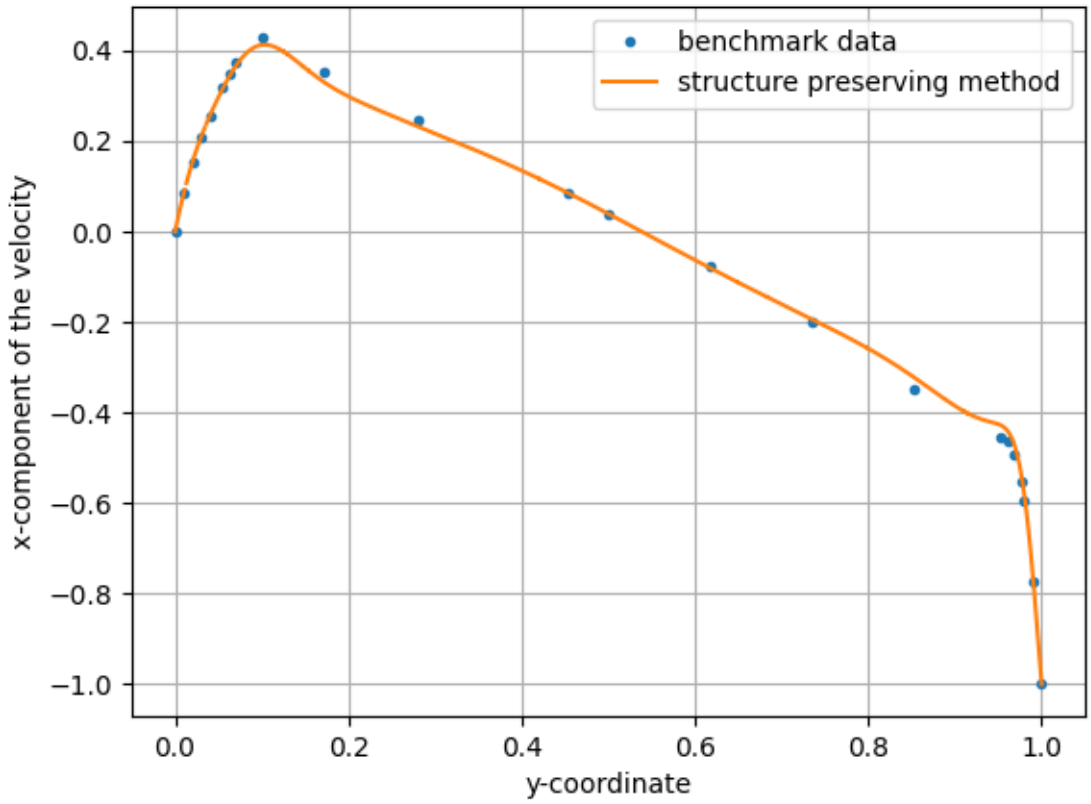

[width=8cm]

Figure 4.6: Comparison of the x-component of the velocity along the line x=0.5 for Re=2500

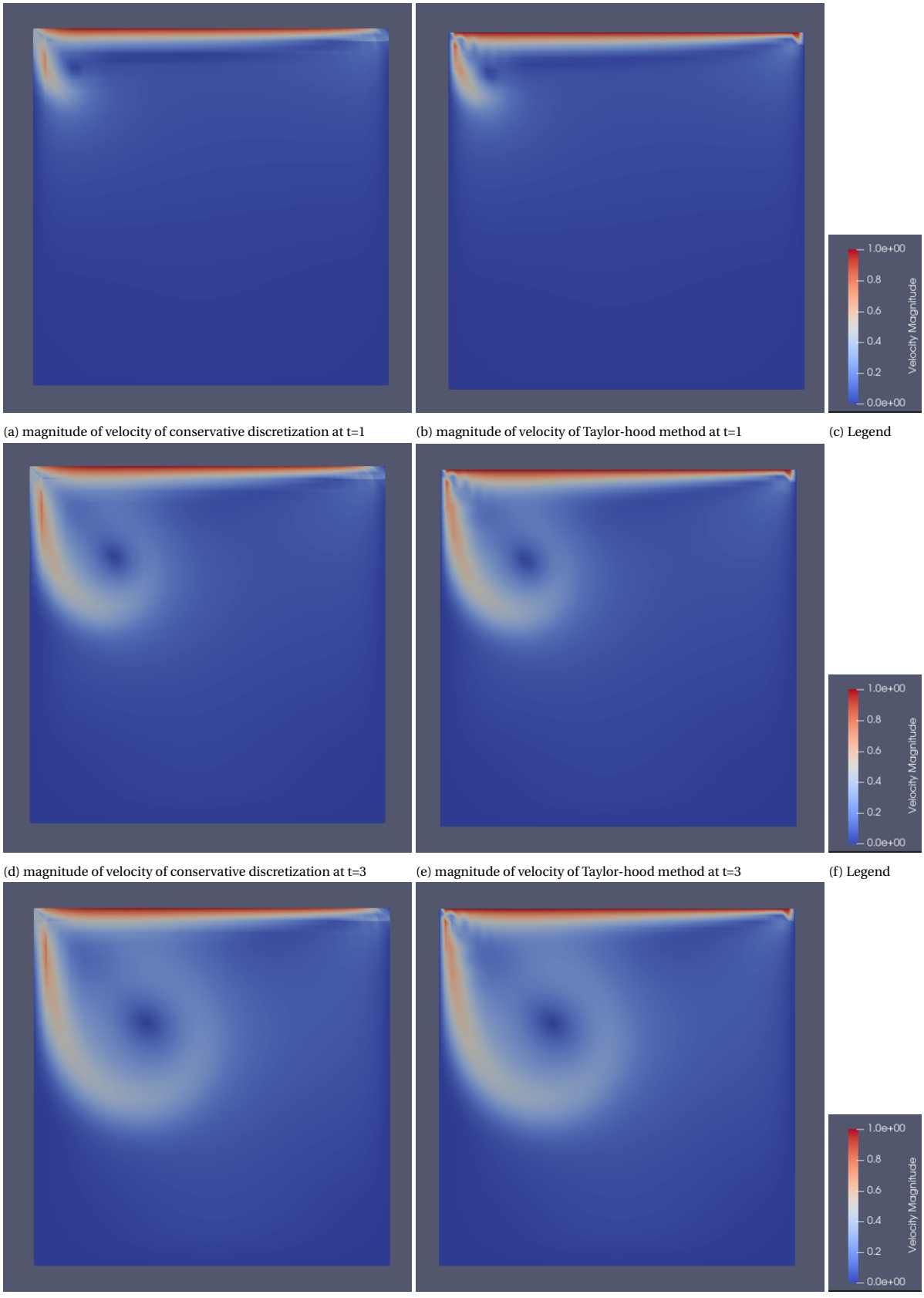

(a) magnitude of velocity of conservative discretization at t=1

(b) magnitude of velocity of Taylor-hood method at t=1

(c) Legend

(d) magnitude of velocity of conservative discretization at t=3

(e) magnitude of velocity of Taylor-hood method at t=3

(f) Legend

(g) magnitude of velocity of conservative discretization at t=5

(h) magnitude of velocity of Taylor-hood method at t=5

(i) Legend

Figure 4.7: Comparison between conservative discretization and Taylor-Hood method for Re=1000, and 28 by 28 mesh and time step 0.01 at times 1, 3 and 5.

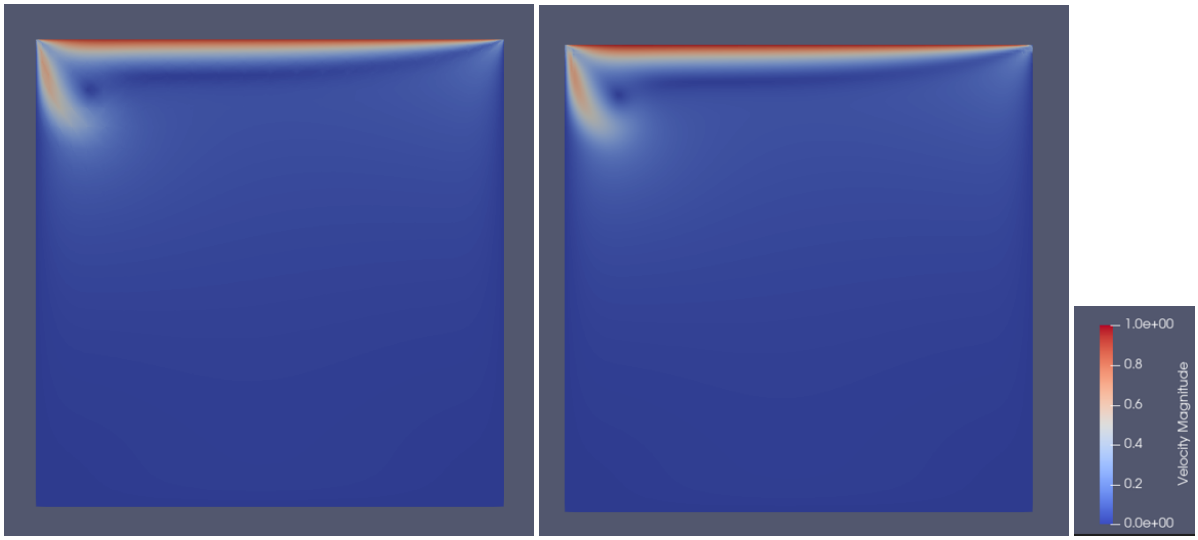

(a) magnitude of velocity on an altered mesh at t=1

(b) magnitude of velocity of the reference at t=1

(c) Legend

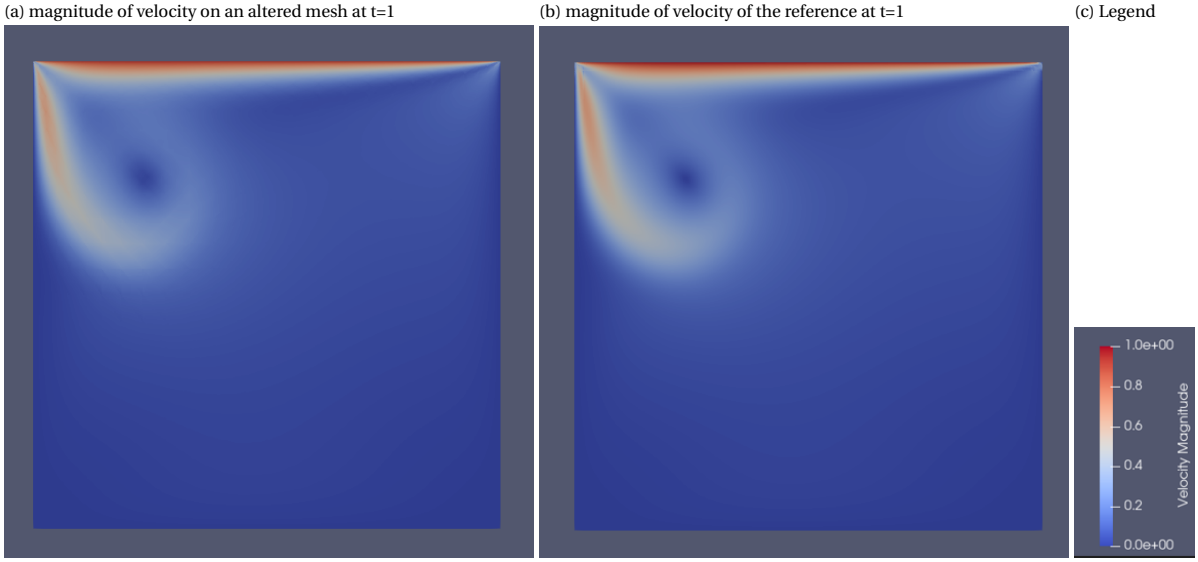

(d) magnitude of velocity on an altered mesh at t=3

(e) magnitude of velocity of the reference at t=3

(f) Legend

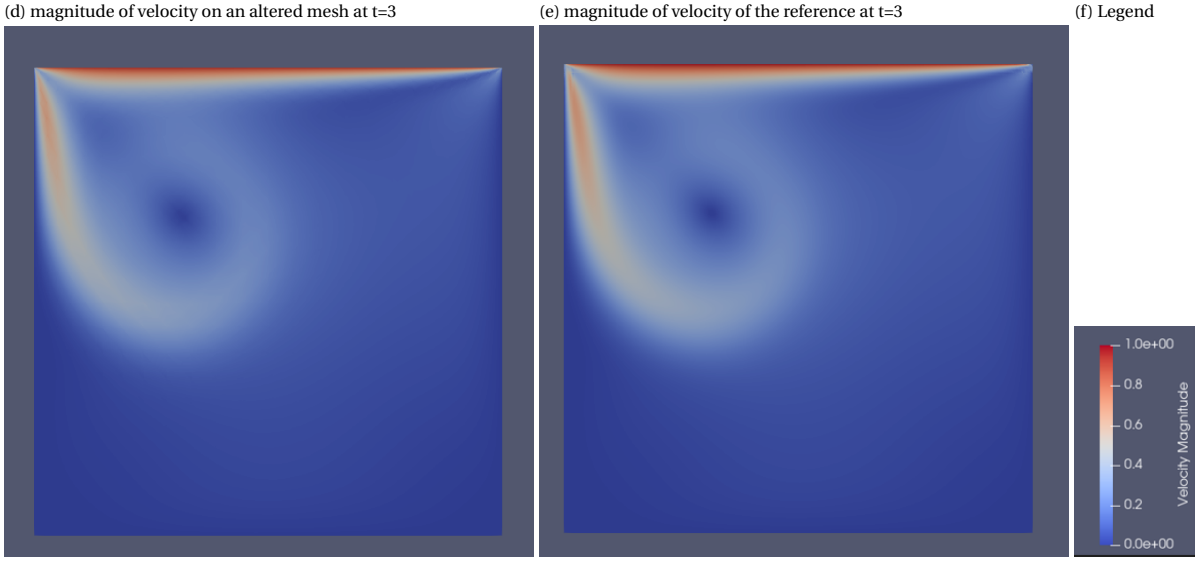

(g) magnitude of velocity on an altered mesh at t=5

(h) magnitude of velocity of the reference at t=5

(i) Legend

Figure 4.8: Comparison between an altered mesh for Re=1000, and 28 by 28 mesh and time step 0.01 at times 1, 3 and 5 and a reference.

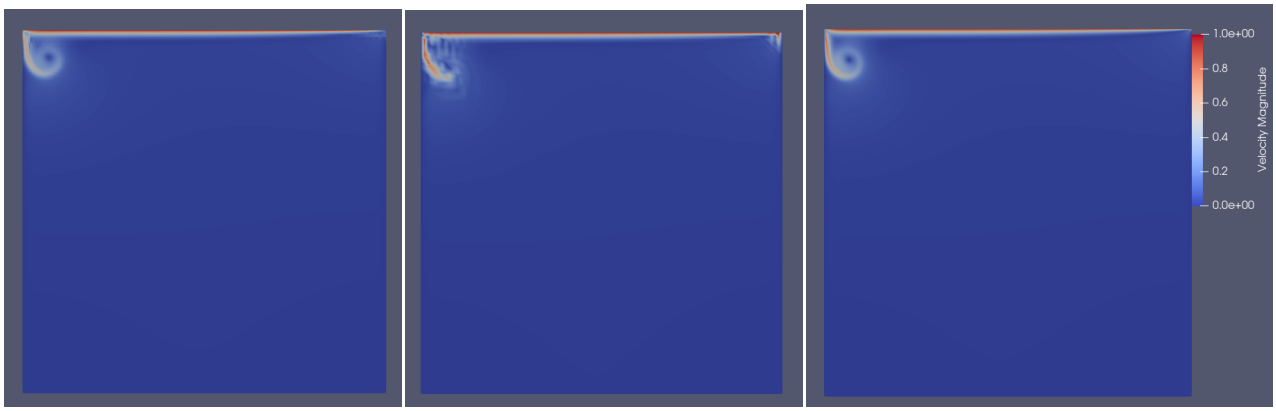

(a) magnitude of velocity of conservative discretization at t=1

(b) magnitude of velocity of Taylor-hood method at t=1

(c) magnitude of the velocity of the higher resolution reference Taylor-Hood

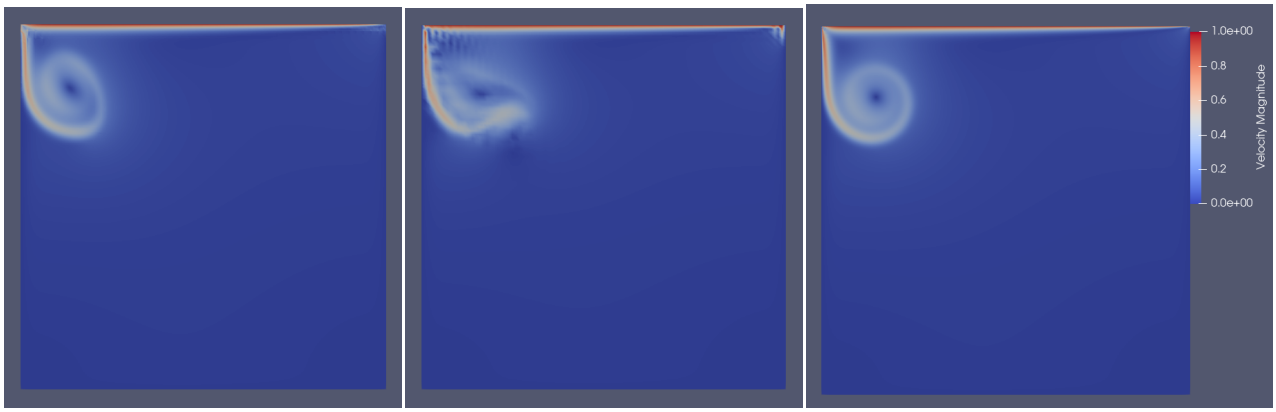

(d) magnitude of velocity of conservative discretization at t=3

(e) magnitude of velocity of Taylor-hood method at t=3

(f) magnitude of the velocity of the higher resolution reference Taylor-Hood

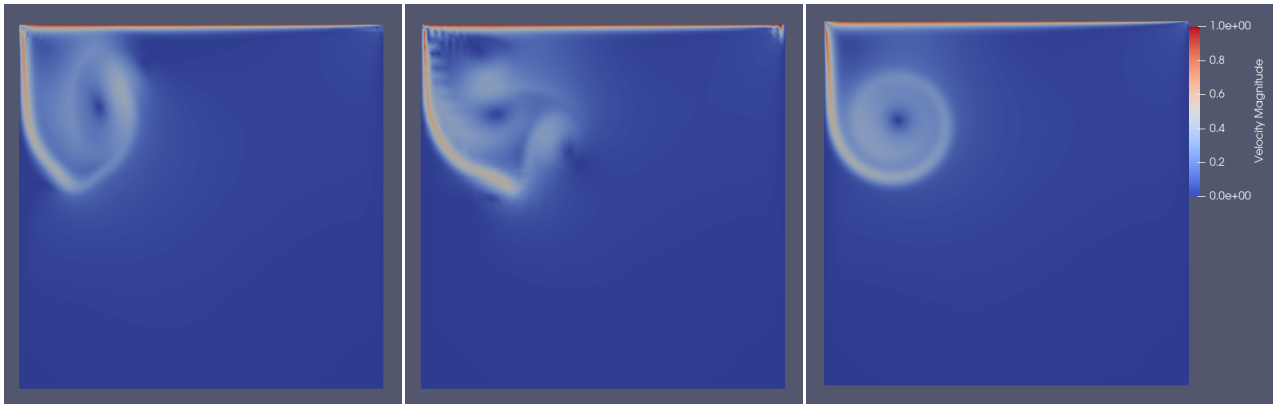

(g) magnitude of velocity of conservative discretization at t=5

(h) magnitude of velocity of Taylor-hood method at t=5

(i) magnitude of the velocity of the higher resolution reference Taylor-Hood

Figure 4.9: Comparison between conservative discretization and Taylor-Hood method for Re=10000, and 50 by 50 mesh and time step 0.01 at times 1, 3 and 5. Also shown is a higher resolved reference with a 200 by 200 mesh.

5

Conclusion

In this report we implement and test a discretization for the 2D dimensionless incompressible Navier-Stokes equations, as described by Zhang, Palha, Gerritsma and Yao [19]. The mass, energy, enstrophy and vorticity conserving discretizations shows results which accurately matches higher resolution benchmark results. For the under resolved case it performed better than the Taylor-Hood method and importantly it did not show any unphysical oscillations in the solution. This result was even more prevalent for the higher Reynolds number case. This clearly shows the utility of this discritisation, since for a lot of practical situations the simulations will be very under resolved.

Due to time constraints, the conservation properties of these equations were not tested. These should be confirmed before any other conclusions are made.

Bibliography

[1] D. N. Arnold, R. S. Falk, and R. Winther. Finite element exterior calculus: From hodge theory to numerical stability. *AMS*, 2009.

[2] S. Badia and F. Verdugo. Gridap: An extensible finite element toolbox in julia. *Journal of Open Source Software*, 5(52):2520, 2020. doi: 10.21105/joss.02520. URL https://doi.org/10.21105/joss.02520.

[3] J. Bezanson, A. Edelman, S. Karpinski, and V. B. Shah. Julia: A fresh approach to numerical computing. *SIAM review*, 59(1):65–98, 2017. URL https://doi.org/10.1137/141000671.

[4] O. Botella and R. Peyret. Benchmark spectral results on the lid-driven cavity flow. *Computers & Fluids*, 27(4):421–433, 1998. ISSN 0045-7930. doi: https://doi.org/10.1016/S0045-7930(98)00002-4. URL https://www.sciencedirect.com/science/article/pii/S0045793098000024.

[5] Capuano and Vallefuoco. Effects of discrete energy and helicity conservation in numerical simulations of helical turbulence. *Springer*, 2017.

[6] M. O. Deville. *An Introduction to the Mechanics of Incompressible Fluids*. Springer, 2022.

[7] M. D. Gunzburger and P. B. Bochev. *Least-squares finite element methods*. Springer, 2009.

[8] D. A. Ham, P. H. J. Kelly, L. Mitchell, C. J. Cotter, R. C. Kirby, K. Sagiyama, N. Bouziani, S. Vorderwuelbecke, T. J. Gregory, J. Betteridge, D. R. Shapero, R. W. Nixon-Hill, C. J. Ward, P. E. Farrell, P. D. Brubeck, I. Marsden, T. H. Gibson, M. Homolya, T. Sun, A. T. T. McRae, F. Luporini, A. Gregory, M. Lange, S. W. Funke, F. Rathgeber, G. Bercea, and G. R. Markall. *Firedrake User Manual*. Imperial College London and University of Oxford and Baylor University and University of Washington, first edition edition, 5 2023.

[9] Hughes and T. J. R. *Finite Element Method - Linear Static and Dynamic Finite Element Analysis*. Dover Publications, 2000. ISBN 978-0-486-41181-1. URL https://app.knovel.com/hotlink/toc/id:kpFEMLSDF1/finite-element-method/finite-element-method.

[10] A. Jameson, L. Martinelli, and N.A. Pierce. Optimum aerodynamic design using the navier–stokes equations. *Springer*, 1998.

[11] J. Jost and X. Li-Jost. *Calculus of Variations*. Cambridge Studies in Advanced Mathematics. Cambridge University Press, 1998. ISBN 9780521642033. URL https://books.google.nl/books?id=QN8Iw7fUA-8C.

[12] A. Logg, K. Mardal, and G. Wells. *Automated Solution of Differential Equations by the Finite Element Method: The FEniCS Book*, volume 84. 04 2011. ISBN 978-3-642-23098-1. doi: 10.1007/978-3-642-23099-8.

[13] F. Mesinger and A. AJakawa. Numerical methods used in atmospheric models. August 1976.

[14] A. Palha and M. Gerritsma. A mass, energy, enstrophy and vorticity conserving (meevc) mimetic spectral element discretization for the 2d incompressible navier–stokes equations. *Journal of Computational Physics*, 2017.

[15] Y. Papadopoulos. URL www.acenumerics.com.

[16] J. Blair Perot. *Discrete Conservation Properties of Unstructured Mesh Schemes*. 2011. URL https://www.annualreviews.org/content/journals/10.1146/annurev-fluid-122109-160645.

[17] C. Susanne, L. Brenner, and S. Ridgway. *The Mathematical Theory of Finite Element Methods*. Springer, third edition, 2008.

[18] F. Verdugo and S. Badia. The software design of gridap: A finite element package based on the julia JIT compiler. *Computer Physics Communications*, 276:108341, July 2022. doi: 10.1016/j.cpc.2022.108341. URL https://doi.org/10.1016/j.cpc.2022.108341.

[19] Y. Zhang, A. Palha, M. Gerritsma, and Q. Yao. A meevc discretization for two-dimensional incompressible navier-stokes equations with general boundary conditions. *Journal of Computational Physics*, 510, 2024. doi: 10.1016/j.jcp.2024.113080. URL https://www.scopus.com/inward/record.uri?eid=2-s2.0-85192739529&doi=10.1016%2fj.jcp.2024.113080&partnerID=40&md5=aac63cea9c59c0443e6686e166ff79e3.